Lithogeochemistry in exploration for intrusion-hosted magmatic Ni-Cu-Co deposits

Stephen J. Barnes

CSIRO Mineral Resources, Perth, WA, Australia

Steve.barnes@csiro.au

This paper is a non-peer reviewed preprint submitted to EarthArXiv

Currently in review for journal Geochemistry: Exploration, Environment, Analysis

Lithogeochemistry in exploration for intrusion-hosted magmatic Ni-Cu-Co deposits

Stephen J. Barnes

CSIRO Mineral Resources, Perth, WA, Australia

Steve.barnes@csiro.au

First submission for GEEA

(Running title Lithogeochemistry for Nickel Exploration)

Abstract

Magmatic Ni-Cu-Co-PGE deposits are notoriously difficult exploration targets owing to a lack of alteration haloes or other extended distal footprints. Success requires prediction of prospective terranes, followed by identification of suitable host intrusions and deposition sites within those intrusions. At the regional scale, potential ore-hosting magmas tend to have lithophile trace element trends falling on mixing lines between primitive or slightly depleted source mantle and typical upper continental crust, with several significant exceptions. Most known deposits have parent magmas that are in the upper range of FeO content for given MgO compared with baseline data sets for continental LIP magmas. At the scale of individual intrusions, the presence of cumulate rocks, both mafic and ultramafic, is key. These can be recognised in regional datasets using combinations of magnesium number (molar MgO/(MgO+FeO), Al_2O_3, TiO_2 and Zr contents. Combinations of alteration-resistant element ratios between Ni, Cr and Ti are also useful and can also be applied to moderately weathered samples. Concentrations and ratios of Cu and Zr are useful in discriminating chalcophile-enriched and depleted magmas suites. In combination, these approaches can be combined to discriminate highly prospective cumulate-dominated magmatic suites and individual intrusions from non-cumulate suites with limited potential.

Keywords: lithogeochemistry, magmatic sulfide, chalcophile elements, nickel, platinum group elements, copper

1 Introduction

Magmatic Ni-Cu-Co deposits hosted in mafic-ultramafic intrusions make up a large proportion of the global sulfide Ni resource endowment, and a large proportion of the global Ni-Co endowment overall (about 37%, based on figures from (Mudd and Jowitt 2014)). One single deposit, the Oktyabrsky system in the Norilsk-Talankh region, includes well over half a trillion dollars' worth of contained metals and a number of other large deposits exceed $100 billion in value (Mudd and Jowitt 2014;

Barnes *et al.* 2020). With the expected increased demand for Ni, Cu and Co in the electric vehicle market, there is a greatly increased interest in exploring for this type of target. This interest has been further sparked by several substantial discoveries in Proterozoic orogenic belts in Western Australia: Nova-Bollinger (Bennett *et al.* 2014), Silver Knight and Mawson in the Albany Fraser Orogen, Julimar (Gonneville) in the Jimperding Metamorphic Belt only 70km from the city of Perth, and the Savannah North discovery in the Halls Creek Orogen (Hicks *et al.* 2017; Le Vaillant *et al.* 2020).

Magmatic sulfide deposits are difficult exploration targets and deposits hosted in small conduit- or chonolith-type intrusions particularly so. The host intrusions in some cases are not much bigger than the deposits themselves (Lightfoot *et al.* 2012), there are no associated alteration haloes, structural controls are typically cryptic and the geological controls on deposition sites are not well understood. Electromagnetic methods are effective but often confounded by the presence of barren conductors such as graphitic schists, and where deposits are steeply plunging or deeply buried their geophysical expression is minimal (Peters 2006). The discoveries at Nova-Bollinger (Bennett *et al.* 2014) and Nebo-Babel hinged on single-point soil geochemical anomalies that could easily have been missed. Successful exploration requires a comprehensive toolkit, of which lithogeochemistry can be a valuable part. In this contribution we concentrate on the application of lithogeochemical and mineral chemistry to exploration for intrusion-hosted Ni-Cu dominant systems, complementing the review pertaining to komatiite-hosted deposits given by (Le Vaillant *et al.* 2016). We take a broadly similar approach to that of Halley (2020) of utilising the typical large multi-element ICP-MS datasets that are now routinely collected during regional exploration programs, asking what kinds of information can be extracted from them, at what scale, and with what degree of confidence. A complementary mineral-chemistry based approach, using the Ni content of olivine, has been assessed in a companion paper (Barnes *et al.* 2022b).

As with komatiite-related targets (Lesher *et al.* 2001; Barnes and Fiorentini 2012; Le Vaillant *et al.* 2016), lithogeochemical exploration takes two distinct but overlapping approaches: prediction, recognising potentially “fertile” host rocks; and detection, identifying the signatures of the ore-forming process. In both cases, but particularly in host rock recognition at the greenfields stage, the imperative is to derive useful information from spatially sparse information. Using that information, we aim to minimise false positives and false negatives at the same time as identifying what might be extremely subtle indicators.

Modern exploration programs collect colossal volumes of geochemical data. Most commercial laboratories now offer ICP-MS or ICP-OES analyses of 40 or more elements per sample, and tens of thousands of samples can be and often are analysed during an extensive exploration program. The key to obtaining the best value from these large datasets lies in using the data to answer specific questions arising from mineral system models (Figure 1). Here are some important ones, in descending order of scale:

1. Are we in a prospective magmatic province where favourable “carrier magmas” are present?
2. Are suitable intrusive bodies present where magmas could carry and deposit sulfide liquids?
3. Is there evidence that the magmas have been interacting with their country rocks along the flow pathway?
4. Are the samples at or close to a deposition site, where suspended silicate crystals are being deposited from the magma to form cumulate rocks?
5. Is there evidence for the presence and/or deposition of sulfide liquid droplets?

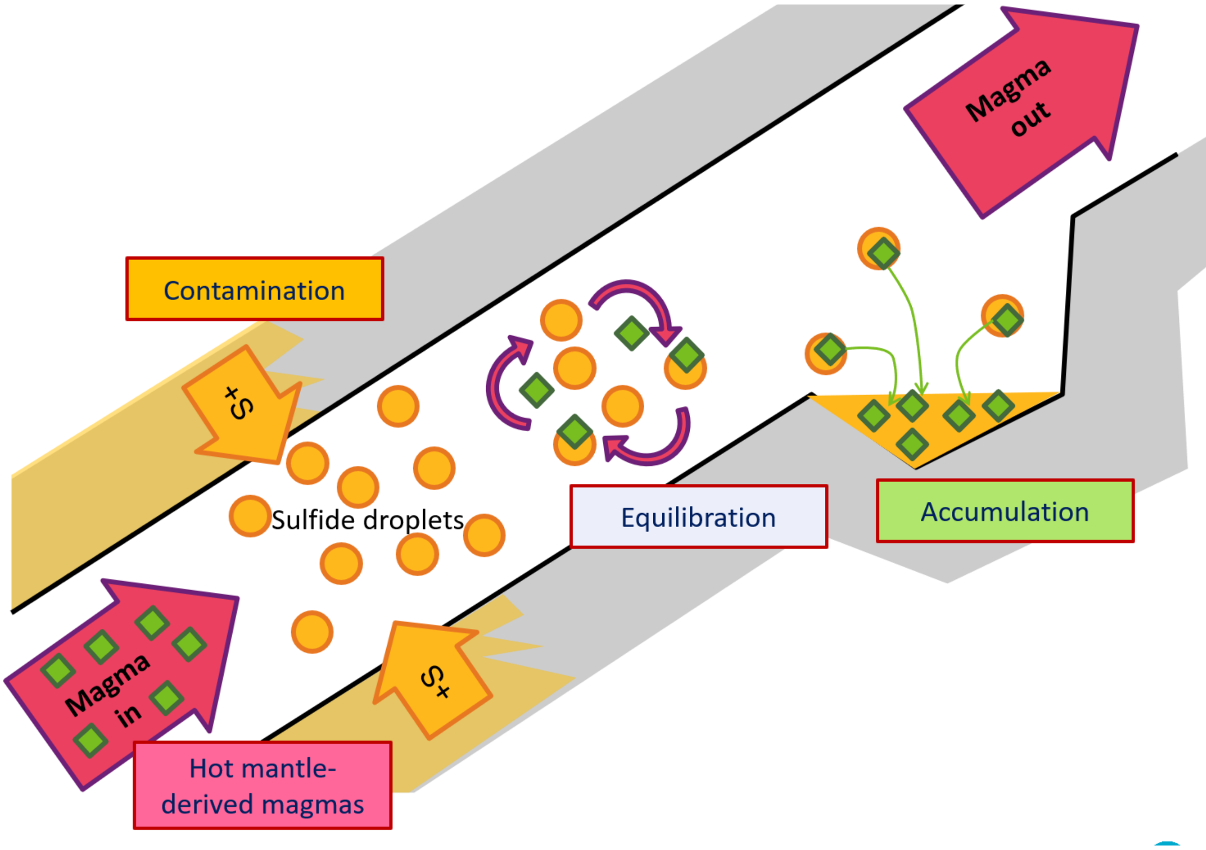

Figure 1, schematic genetic scheme for Ni-Cu dominant magmatic sulfide ore deposits.

Clearly if the answer to the last question is positive, this is by far the best geochemical indicator of magmatic ore formation and a viable target has been identified. But there are many examples of near-misses where lack of evidence of sulfide in rocks from an unmineralized part of an ore-bearing intrusive system could generate a false negative. Furthermore, signals of country rock interaction, in the form of geochemical indicators of wall-rock contamination of the magma, can be flushed out by uncontaminated fresh magma within the flow pathways. On the other hand, there are very few, if any, examples of ore forming systems where there is not a positive answer to both questions 4 and 5. The geochemical proxies for these five questions are considered, with the aim of producing and explaining some simple and reliable discriminant plots of practical use in exploration industry.

2 Classification and Genetic models

2.1 Classification of deposit types

Numerous classification schemes have proposed over the years, of which that of Naldrett (2004) is the most widely adopted. For the purposes of this contribution, we start with a simple scheme that uses a combination of two orthogonal variables: tectonic setting, and the scale of the host intrusion, distinguishing between, on one hand, large layered mafic-ultramafic intrusions with 1km or greater thickness of cumulate rocks and, on the other, small intrusions with dimensions of tens to hundreds of metres displaying a variety of geometric forms (Barnes *et al.* 2016a). The common feature of all host intrusions is that they contain a component of cumulate rocks.

Considering tectonic setting first, most known deposits occur within either

1. Intracontinental Large Igneous Provinces (LIPs), generally regarded as being related to mantle plumes, and specifically to the arrival of the heads of starting plumes (Richards *et al.* 1989; Campbell and Griffiths 1990), of which the Siberian LIP is the prime example; large layered mafic-ultramafic intrusions such as the Bushveld Complex are included in this setting; and
2. Orogenic belts representing continental collisions and continental arcs, relating to mafic magmatism generated at convergent margins. A caveat is needed here in that in some cases "orogenic belt" localities may be sampling plume magmas emplaced along craton margins and caught up in collisional events, such as Wrangellia in the North American Cordillera (Lassiter *et al.* 1995); this is particularly an issue in highly deformed Proterozoic orogens such as the Albany-Fraser Orogen in Western Australia (Smithies *et al.* 2013; Spaggiari *et al.* 2015). For purposes of this study, we include all such occurrences in the Orogenic Belt category but acknowledge the strong possibility of misclassification.

Within LMI's, there are four predominant modes of occurrence of magmatic sulfide mineralisation:

1. stratiform low-S PGE-dominant mineralisation within a layered cumulate sequence, such as the Merensky Reef, JM Reef and UG2 chromitite (Mungall and Naldrett 2008);
2. low-S PGE-dominated deposits within marginal rocks of which the Platreef is the prime example (Kinnaird *et al.* ; McDonald and Holwell 2011; Barnes *et al.* 2017a);

3. thick accumulations of relatively PGE-poor disseminated sulfide within layered cumulates such as in the Duluth, Mirabela and Kevitsa intrusions (Ripley *et al.* 1998; Barnes *et al.* 2011; Santaguida *et al.* 2015); and
4. relatively uncommon basal accumulation of sulfide-rich ores as the Nye Basin occurrence in the Stillwater Complex (Helz *et al.* 1985; Zientek *et al.* 1989).

The latter two styles have most of their value in Ni and Cu rather than PGEs and are therefore considered in this study. In all known cases, large layered mafic intrusions (LMIs) are regarded as being components of continental LIPs, giving us three categories of intrusion hosted Ni-Cu-Co dominant deposit: LMIs, small intrusion hosted deposits in orogenic belts, and small intrusion hosted deposits in continental LIPs. Having made that distinction, the question arises of whether the types of small-intrusion hosted deposit found in these two settings are actually systematically different. Considering the types of intrusions that host deposits (Lightfoot and Evans-Lamswood 2015; Barnes *et al.* 2016a; Barnes and Mungall 2018) the answer is probably no. The various types of ore-hosting small intrusions including chonoliths and blade-shaped dykes (Barnes and Mungall 2018) are equally likely to be found in either setting. Therefore for the purposes of prospect-scale exploration the distinction is not particularly useful, and it is more useful to consider deposit types in terms of the nature of the host intrusion and the mode of occurrence of the sulfide accumulation, following the scheme commonly used for komatiite-associated deposits (Barnes 2006; Lesher and Barnes 2008).

Within small intrusions, there is similarly a spectrum of occurrences from

1. dispersed disseminated ores within the interior of intrusions lacking sulfide-rich basal accumulations, examples being Jinchuan (Mao *et al.* 2018) and Xiarihamu (Tibet) (Li *et al.* 2015b; Song *et al.* 2016a), the equivalent of Type 2 deposits in komatiites, to
2. sulfide-rich ores dominated by massive, semi-massive and net textured ores (Barnes *et al.* 2018) usually but not exclusively at (or below) the basal contact; the equivalent of Type 1 deposits in komatiites. This category includes the major Norilsk-Talnakh deposits.

The intrusive hosts in orogenic and LIP settings share many common characteristics (Barnes *et al.* 2016a), but the geochemical characteristics of the parent magmas may differ considerably. This is significant in defining the geochemical baseline against which to assess prospectivity and targeting criteria. In the following discussion we focus primarily on the application of lithogeochemistry to exploration for Ni-Cu dominated as opposed to PGE-dominated deposits, with a consequent emphasis on small intrusions.

2.2 Genetic models and geochemical consequences

The prime mechanism for formation of Ni-Cu-PGE dominated magmatic sulfide ores (Fig. 1) has been generally agreed upon for several decades (Keays 1995; Barnes and Lightfoot 2005; Naldrett 2011; Barnes *et al.* 2016a).

The essential elements are a (1) magma passing through some kind of trans-crustal conduit system, assimilating S, usually in the form of sulfide, from the country rocks; (2) the sulfide melt so-formed reacting with the carrier magma to become enriched in chalcophile elements; (3) a physical mechanism of segregation and accumulation of the sulfide liquid; and a (4) variety of physical processes including re-entrainment, gravity flow, country rock infiltration and in some cases tectonic mobilisation giving rise to the final disposition of the ores (Barnes *et al.* 2017b; Barnes *et al.* 2018). Of these processes, summarised in Figure 1, the first three all potentially leave geochemical imprints in the host rocks and magmas that are potentially detectable and mappable as exploration proxies at a range of scales. However, the extent to which these proxies are reliable, in terms of false positive and false negative rates, depends on proper understanding of the length- and time-scales at which the various component processes operate and interact (Barnes and Robertson 2019).

In the following discussion, we consider a variety of possible geochemical proxies, from regional to local scale, and assess their applicability and reliability.

3 Identifying prospective host rocks

3.1 "Fertile magmas"

At the largest scale of exploration targeting and terrane selection, an approach widespread in economic geology is the identification of "fertile" magmas. The concept of "fertility" – the capacity of a particular magmatic suite or episode to form ore deposits – has been successfully applied in porphyry Cu exploration (e.g. (Hao *et al.* 2017; Xu *et al.* 2021)) and has proved to have some, albeit limited, application in komatiite-associated Ni-Cu dominant magmatic sulfide mineral systems.

In the case of the komatiite association, the strongly endowed East Yilgarn province of Western Australia has some distinctive geochemical attributes, notably a strong signal of crustal contamination and a preponderance of highly magnesian olivine-rich cumulates compared with less-endowed provinces such as the Abitibi belt (Barnes *et al.* 2007; Barnes and Fiorentini 2012). However, these geochemically detectable signals are regarded as a consequence of a craton-margin tectonic setting (Begg *et al.* 2010; Mole *et al.* 2014) and presence of favourable volcanic facies (Barnes and Fiorentini 2012; Gole and Barnes 2020) rather than an input of particularly "fertile" magma; very similar source magmas exist in the Abitibi and numerous other much less endowed greenstone belts.

A corresponding global data analysis for deposits associated with mafic magmas (as opposed to komatiites) is more challenging, the main reason being that, unlike in komatiite terranes, unambiguous parent magmas to the host bodies are only rarely available for sampling. There are exceptions, on situations where prospective intrusive bodies and overlying volcanic equivalents are both preserved within continental large igneous provinces, e.g. the Siberian Traps in the Norilsk-Talnakh region (Lightfoot *et al.* 1990; Naldrett *et al.* 1996c) and the Mid-Continent Rift of central North America (Keays and Lightfoot 2015). In other provinces, the geochemical character of the parent magmas have to be inferred indirectly from the intrusions themselves, with complications due to local scale wall-rock contamination and disruption of primary magmatic signals by cumulus processes. In many exploration campaigns, particularly at the early greenfields stage, it is likely that most of the available geochemical information will come from sparsely sampled intrusive rocks, so it is useful to consider how much "fertility" information can be extracted from such sampling. We consider two aspects: firstly, the various lithophile and chalcophile trace element signatures that have been considered indicative of particular tectono-magmatic settings, and secondly the range of MgO contents (and hence temperature) of parent magmas inferred from whole rock data and mineral chemistry.

3.1.1 Lithophile trace elements

The first approach is to use alteration-immobile incompatible trace elements and ratios in magmas on a regional scale. (Zhang *et al.* 2008) and (Griffin *et al.* 2013) analysed a large trace element and isotopic database of flood basalt compositions and clamed to discern a distinctive signal of "fertile" magmatism attributable to the involvement of lithospheric mantle sources. The distinction is subtle at best, and rests heavily on the identification of the Karoo LIP as being fertile on the evidence of a single very minor occurrence in the Insizwa intrusion (Lightfoot and Naldrett 1984), as well as the inclusion of a number of LIPs that have not been extensively explored or not explored at all. This claim has been criticised on these and other grounds by (Arndt 2013). Here I further test the concept using a suite of lithophile and chalcophile trace elements from the extensive database of (Barnes *et al.* 2021a) and (Barnes *et al.* 2015), starting with lithophile trace elements. Chalcophile elements are discussed below.

The elements Nb, Yb, Th and the REE, along with Zr and Y, are commonly used as petrogenetic proxies and as indicators of tectonic setting. The latter application has been heavily criticised by a number of recent publications (Condie 2015; Li *et al.* 2015a; Barnes *et al.* 2021a), but the relative proportions of these elements are nonetheless important indicators of petrogenetic processes. Barnes et al. (2021b) show that most of the useful variance in the entire suite can be captured in the commonly used plot of Th/Yb vs Nb/Yb devised by Pearce (Pearce 2008, 2014) and we apply that approach here. Given that many of the samples used in this exercise are cumulates (see below), it is necessary to apply some filters to eliminate the effect of crystal accumulation on the ratios so the sample set is restricted to exclude orthocumulate and mesocumulate rocks by filtering out samples with <0.5 ppm Th or <0.5 ppm Nb (see Appendix of Barnes et al., 2021b for a full discussion).

The Th-Nb-Yb signature of continental LIPs and their Archean and early Proterozoic equivalents has changed gradually through Earth history (Barnes et al., 2021). The signature of Archean and early Proterozoic volcanic sequences, mineralised or not, is a consistent broadly linear trend ranging from primitive to slightly depleted mantle along a steep trend of variable Th/Nb ratio representing mixing of mantle melts with continental crust (Figure 2 A), and generally lacking the linear trend of constant Th/Nb from depleted MORB to OIB mantle, the "mantle array" of Pearce (2008) (Figure 2). The early Proterozoic terranes of the northern Fennoscandian shield, specifically the mineralised Pechenga belt (Green and Melezhik 1999; Brugmann *et al.* 2000; Latypov *et al.* 2001; Hanski *et al.* 2011) (Figure 2B) are an important exception. In contrast, Phanerozoic LIPs such as the Emeishan and Siberian flood basalt provinces (Figure 2C,D,E) are best represented as mixtures of magmas derived along the length of the mantle array with continental contaminants. The mantle array component appears gradually in the geological record, first appearing clearly in the Early Proterozoic and becoming dominant by around 1100 Ma as represented by the Mid Continent Rift of North America (Figure 2). (A more comprehensive dataset and some additional plots incorporating other lithophile elements are available in the supplemental materials).

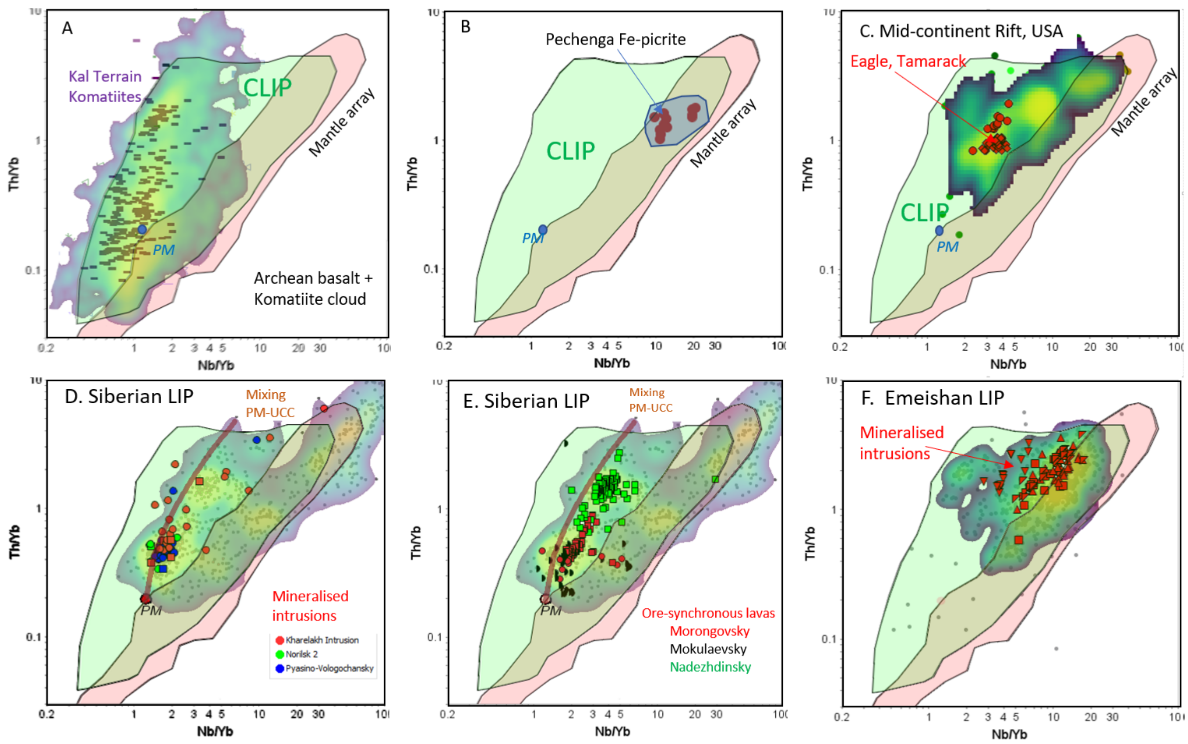

Figure 2. Pearce Th/Yb vs Nb/Yb plot for selected LIPs. A, Archean komatiites from the Kalgoorlie Terrane, Western Australia, over the data cloud for all Archean basalts and komatiites, superimposed on the 80th percentile outline for all continental LIP basalts (CLIP) and all non-arc oceanic basalts that define the "mantle array, based on the data compilation of Barnes et al. (2021b). B, CLIP and mantle array field with data points for "ferropicrites" from the Pechenga Belt of the Baltic Craton. This is the only Archean or PaleoProtoerozoic mineralised belt where mineralisation is associated with magmas at the high Nb/Yb end of the mantle array. C, data cloud for basalts from the Mid Continent Rift of the USA, along

with data points for samples of two mineralised conduit systems in the Rift, Eagle and Tamarack. D,E, data cloud for the Siberian LIP. D includes data points for three of the mineralised intrusions, E for basalts from the three groups considered to be spatially and/or temporally associated with the ore forming event. Mixing PM-UCC is the trajectory for contaminating a basalt with primitive mantle (PM) ratios with average upper continental crust. F, data cloud for the Emeishan LIP, along with data points from mineralised intrusions. Data sources: Table 1

For the two most extensively mineralised LIPs, the Mid-Continent Rift of the USA, containing Eagle, Tamarack and the very large but very low grade deposits of the Duluth Complex (Figure 2C), and the Siberian LIP (Figure 2D,E), the mineralised intrusions tend to fall toward the low Nb/Yb end of the array for the LP as a whole, and have patterns broadly consistent with upper crustal contamination of primitive mantle-derived basalt ("Mixing PM-UCC" in Figure 2), i.e. similar to those seen in Archean komatiite-basalt suites. The same is true of the three units of the Siberian flood basalt sequence that are thought to be temporally and spatially most closely associated with the Norilsk-Talnakh ores (Figure 2 E). The final plot in Figure 2 shows the data cloud from the sparsely mineralised Emeishan LIP, along with the data from hosts to several of the small Ni-Cu and PGE sulfide deposits known in the province. There is a clear difference from Siberia and the MCR, but a closer affinity with Pechenga, in that the province as a whole is deficient in the low Nb/Yb component and is dominated by material plotting towards the high Nb/Yb end of the mantle array. It is noteworthy that the SLIP also contains a high proportion of magmas plotting along the mantle array towards high Nb/Yb, but known mineralisation is associated with magmas falling close to the PM-UCC mixing line.

Data on Proterozoic orogenic belts such as the Halls Creek orogen (HCO) (Le Vaillant *et al.* 2020), and the Fraser Zone of the Albany-Fraser Orogen (AFO) (Maier *et al.* 2016; Taranovic *et al.* 2022) show variable distributions (Figure 3). The HCO data overlaps the indistinguishable continental arc and continental LIP field, whereas the AFO data matches more closely with typical Archean basalt-komatiite patterns with a population extending into the modern oceanic arc field, above the mantle array in the lower left of the diagram. In both, the mineralised intrusions define a narrower trend parallel to the Primitive Mantle – Upper Continental Crust (PM-UCC) mixing line, but somewhat to the low-Nb/Yb side of it in the Nova case. Broadly similar trends parallel to the PMM-UC mixing trend are shown by the host intrusions to Jinchuan, Xiarihamu and various deposits of the Central Asia Orogenic Belt in NW China. The main exception is Kalatongke, which also show a parallel trend, but significantly displaced to higher Nb/Yb implying a distinctly e-MORB-type mantle source (Fig. 3E). The displacement of the other CAOB deposits and Xiarihamu towards lower Nb/Yb may indicate a metasomatized arc mantle source contribution consistent with previous interpretations (Lu *et al.* 2019).

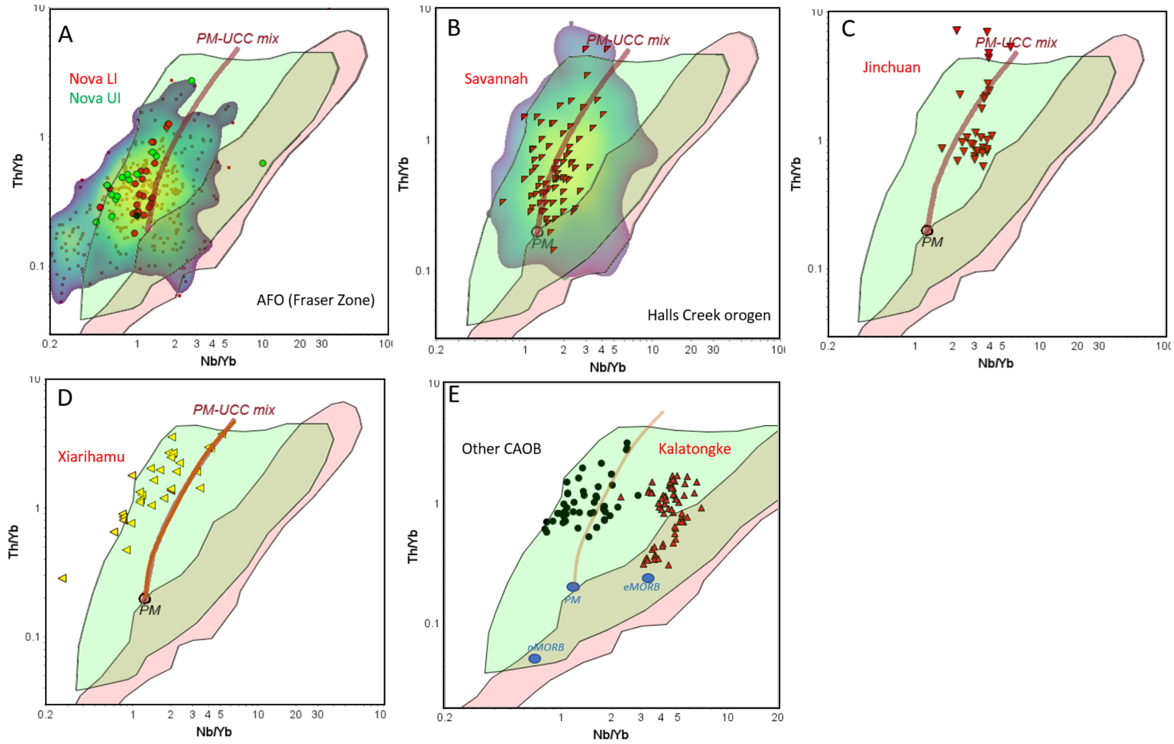

Figure 3. Pearce trace element ratio-ratio plots for intrusion-dominated orogens and host intrusions. A, Nova-Bollinger Upper and Lower (ore-hosting) intrusions compared with background in the Fraser Zone of the Albany-Fraser Orogen in Western Australia; B, Savannah and Savannah North host intrusions compared with background in the Halls Creek Orogen; C, Jinchuan deposit, Gansu, China; D, Xiarihamu deposit in the Kunlun orogenic belt, Tibet; E, Kalatongke deposit, Central Asian Orogenic Belt (CAOB), Xinjiang, China and other deposits in the CAOB. "PM-UCC mix" is the trajectory for contaminating a basalt with primitive mantle (PM) ratios with average upper continental crust. Data sources: Table 1. Data filtered to eliminate samples with <0.5 ppm Th and <0.5 ppm Nb to eliminate adcumulates and mesocumulates.

In conclusion, here is some evidence to suggest that magmas with trace element compositions falling close to mixing lines between primitive mantle and average continental crust, the characteristic variable Nb/Th trend, have a greater tendency to occur in ore-bearing terranes and to be responsible for ore formation. The Mr-Mk suite of the Siberian Traps is the type example of this "sweet spot". The main outlying exception is the Pechenga belt in far north-western Russia (Green and Melezhik 1999; Brugmann *et al.* 2000; Latypov *et al.* 2001; Hanski *et al.* 2011), where the unusual ferropicrite magmas have trace element characteristics very similar to the ocean island end of the mantle array (Hanski *et al.* 2011). It is likely that they were derived a highly anomalous region of source mantle (Hanski and Smolkin 1995). This approach, while indicative, does not lead to a single reliable discriminant of "fertile" magmas.

3.1.2 Chalcophile element depletion as a regional footprint

The chalcophile element contents, particularly the platinum group element contents, of mantle derived and ore-associated magmas has been extensively reviewed, for komatiites by (Fiorentini *et al.* 2010; Fiorentini *et al.* 2011) and for basaltic magmas by Barnes et al. (Barnes *et al.* 2015). The potential association of PGE depleted basalts with the super-giant Ni-Cu-PGE deposits of the Norilsk-Talnakh camp has been identified in a number of studies (Brugmann *et al.* 1993; Naldrett *et al.* 1996b;

Lightfoot and Keays 2005) and was widely assimilated into exploration strategies in the 1990s, but there is ongoing debate about whether the association is purely coincidental (Arndt 2011) or genetically related by complex sequences of events e.g. (Li *et al.* 2009; Yao and Mungall 2021). Taking a purely empirical view, Norilsk-Talnakh remains to this day the only example in a mafic magmatic system where a clear spatial relationship exists between mineralised intrusions and PGE depleted lavas, although it is now generally agreed that the lavas in question are slightly older than the intrusions e.g. (Latyshev *et al.* 2020) and are geochemically not directly related to the intrusions (Latypov 2002). In most cases elsewhere, it is not possible to sample rocks that demonstrably represent the parent magmas to ore-hosting intrusions; either they are contaminated by wall rocks in the margins of the intrusions, or they have been eroded away. Hence the applicability of chalcophile element depletion to fertility analysis of a particular terrane is limited in most cases. The plume-related Tertiary provinces of east and west Greenland may be exceptions, where intrusions can be recognised in the basement to a lava pile containing PGE-depleted basalts (Keays and Lightfoot 2007).

The applicability to mafic-related systems in orogenic belts is complicated by the possibility that mantle derived magmas may be relatively low degree partial melts that were sulfide-saturated at source and hence left PGEs in the mantle. This effect is seen in the tendency of lower MgO basalts to have a wider spread of PGE contents towards lower values (Barnes et al., 2015, 2016), and also in magmatic sulfide deposits in orogenic settings typically having significantly low PGE contents over a similar range of Ni (Figure 4). Consequently, PGE depletion is not a reliable signal of ore formation in orogenic settings.

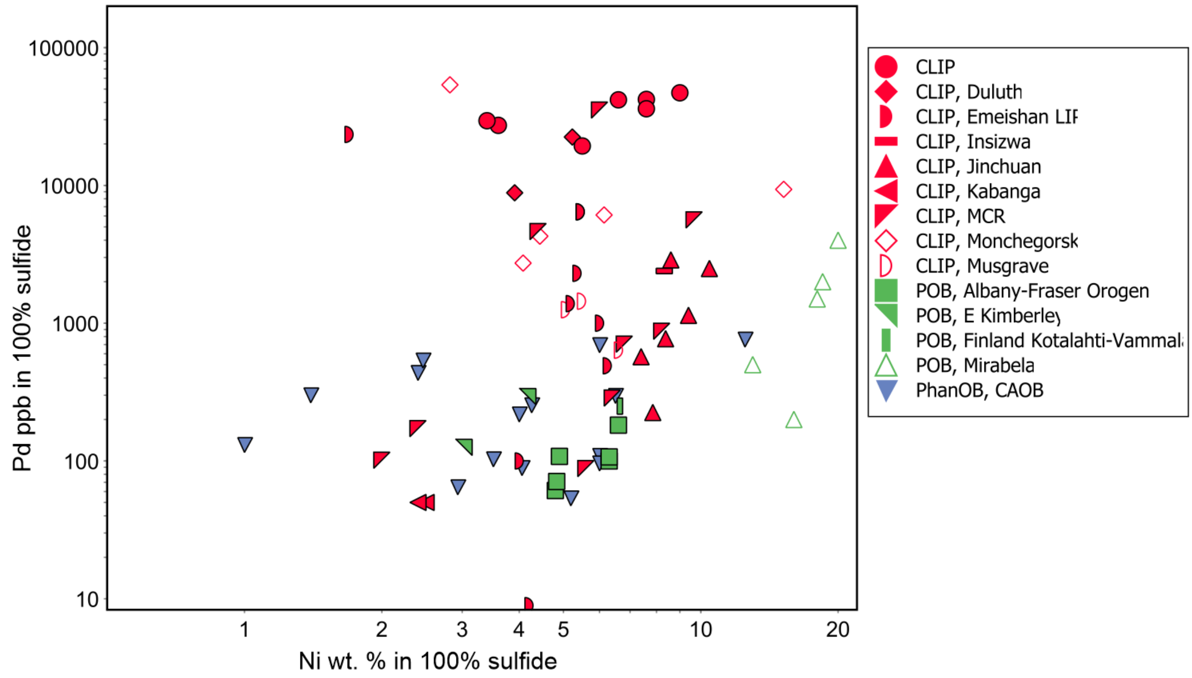

Figure 4. Tenors in ore deposits in mafic-dominant intrusive systems, by setting. CLIP = continental large igneous province, POB = Proterozoic orogenic belt. CAOB = Central Asian Orogenic Belt, NW China. Data sources: (Mudd and Jowitt 2014; Barnes et al. 2017a; Lu et al. 2019).

3.2 Finding hot magmas

It is widely believed principle that magmatic sulfide ores are preferentially associated with high-MgO rocks and therefore by inference high-temperature magmas. This is intuitively obvious: high-temperature, high-MgO magmas have a greater potential to assimilate their country rocks, and hence to achieve the first stage of sulfide melt formation. However, applying this principal is complicated by the fact that in exploration contexts we only rarely (if ever) sample liquids, and most of the rocks we analyse are liable to be cumulates. As discussed below, the MgO content and the Mg/Fe ratio of an ultramafic cumulate rock is inevitably higher than that of the magma it formed from.

3.2.1 Major elements: Olivine as an MgO/T proxy

In the present context of fertility, a better index of the temperature of the ore-forming magma is the Mg number [molar [Mg/(Mg+Fe)] of the most common associated cumulus silicate mineral in such systems, olivine.

A compilation of the range of measured olivine compositions (expressed as molar percent forsterite content, Fo, the same thing as the Mg number) is shown in Figure 5, for small intrusions with basaltic to high-Mg basaltic parent magmas. Fo in olivine shows a very wide range between high values around 90 (implying high-Mg basaltic parents) and low values of less than 50 implying relatively low-T, evolved magmas. One of the larger deposits in this class, Voisey's Bay, has among the least forsteritic olivines. On these empirical grounds, Mg numbers and olivine compositions do not appear to have a great deal of predictive or discriminant ability in Ni sulfide systems. It is probably true (although untested) that within any give province the most Mg-rich olivines are most likely to be associated with ore, but this is not an a priori predictor between provinces. A detailed analysis of olivine compositions in relation to mineralisation is provided by Barnes et al. (2022b).

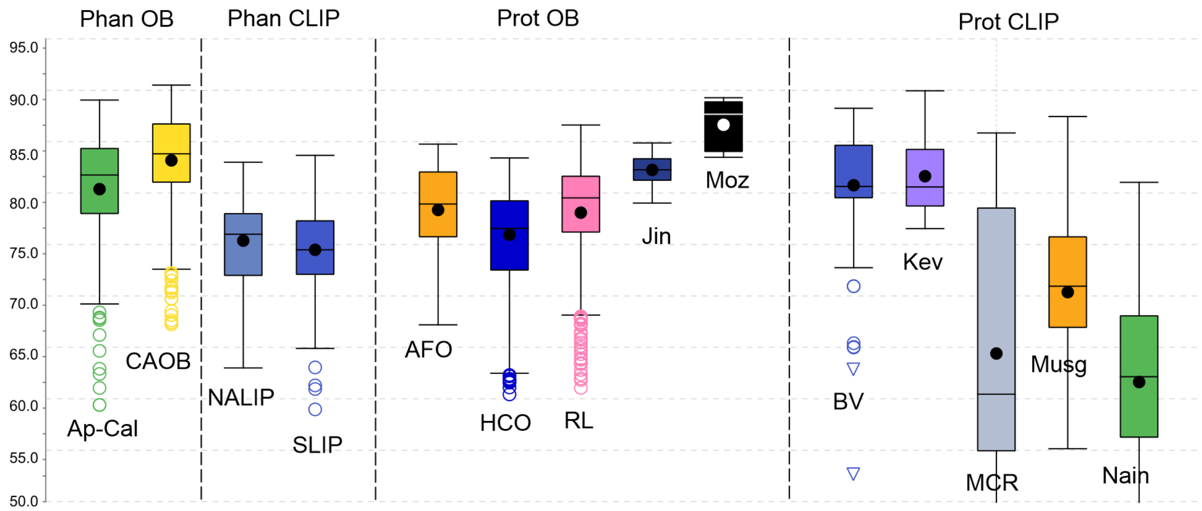

Figure 5 Tukey Box-and-whisker plot of olivine compositions in intrusions in selected Phanerozoic (Phan) and Proterozoic (Prot) continental large igneous provinces (CLIPs) and orogenic belts (OB). Ap-Cal – Apallachian-Caledonide Orogenic Belt (USA and Norway), CAOB – Central Asian Orogenic Belt (NW China), NALIP = North Atlantic LIP (mainly Rum), SLIP = Siberian LIP, AFO = Albany-Fraser Orogen (Australia), HCO = Halls Creek Orogen (Australia), RL = Raahe-Ladoga (Svecofennian) Orogen, Jin = Jinchuan, Moz = Mozambique Mobile Belt (Ntaka Hill), BV = Bushveld Complex, Kev = Kevitsa Intrusion (Finland), MCR = Mid-Continent Rift LIP (USA, Canada), Musg = Musgrave Province (Australia), Nain = Nain Plutonic Suite (E Canada).

3.2.2 Major elements: MgO and FeO in parent magmas

Several studies over the years have suggested that a class of mafic to ultramafic magma called "ferropicrite" may be preferentially associated with magmatic Ni-Cu deposits (Lu *et al.* 2019). This is undeniably true for the Pechenga deposits in NW Russia (Hanski *et al.* 2011), although as we have seen these are highly distinctive in their trace element chemistry compared with other mineralised magma suites. The definition of ferropicrites is not consistently agreed upon, but essentially they represent magmas with moderate to high MgO (10-20%) and high FeO (>12%) (Figure 6). Regardless of the definition, it is of interest in the context of fertility to investigate whether FeO as well as MgO contents of parent magmas may be of interest.

As previously noted, direct determination of parent magmas to intrusions is fraught with difficulty, but some estimates can be made where olivine cumulates of variable composition can be recognised within an intrusion. This method assumes that a suite of rocks exists which can be represented as mixtures of olivine with more or less constant composition and variable proportions of liquid, also of constant composition, in equilibrium with that olivine. The requires a number of steps, described in detail in the supplementary section. This method was first used in the present context for the Jinchuan intrusion (Chai and Naldrett 1992) and has since been used in a number of studies, most recently (Taranovic *et al.* 2022) for the host intrusions to the Nova-Bollinger deposits.

A summary of parent magma estimates for a variety of intrusion-hosted deposits and potentially associated mafic volcanic suites is shown in Figure 6. Generally MgO contents of ore-forming magmas are towards the high end of the field for continental flood basalts in both MgO and FeO, but below the range of the distinctive ferropicrites assumed to be the parent magmas of the Pechenga orebodies. They all fall outside the main cluster for continental arc basalts. The natural range is wide, and several deposit (Norilsk-Talnakh, Savannah, Voisey's Bay, Huangshandong) have unexceptional parent magmas well within the typical range of continental plume magmas. However, there does appear to be threshold MgO-FeO liquid composition curve (red dashed line in Figure 6) below which none of the deposits represented here fall. This lends some support to the idea that deep-seated Fe- and Mg-rich plume magmas (Herzberg *et al.* 2007) are "fertile" and that FeO-MgO whole-rock relationships may be at least moderately diagnostic. A combination of liquid Fe enrichment for given MgO together with lithophile trace elements appears promising as a fertility indicator.

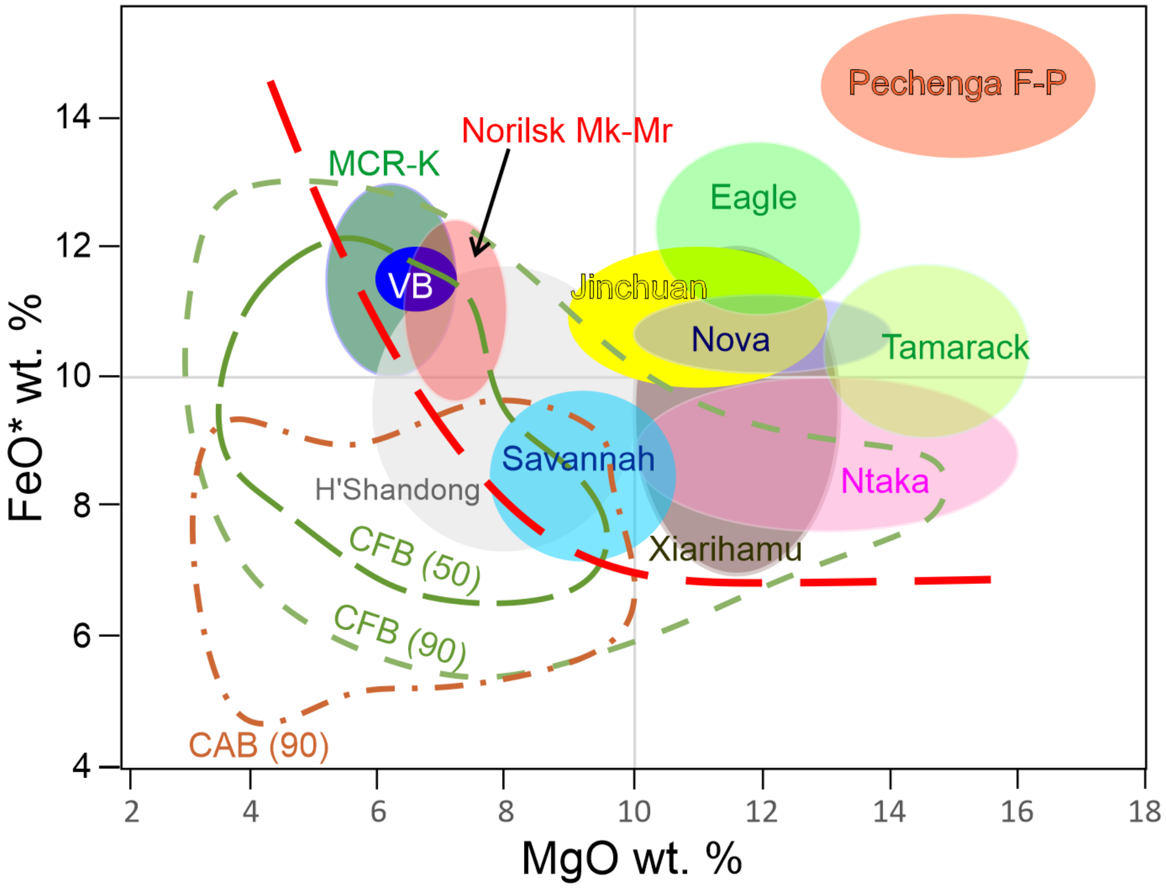

Figure 6. Estimated MgO and FeO contents of parent magmas to various mineralised intrusions (see Table 1 for data sources), compared with 50th and 90th percentile kernel data density on Continental Flood Basalts (CFB) and 90th percentile kernel data density on Continental Arc Basalts from compilation of Barnes et al. (2021), and range of ferropicrites compositions from the Pechenga belt. FeO* is calculated as 90 molar % of total Fe. Norilsk Mk-Mr is the range for the Mokolaevsky and Morongovsky Formations of the Siberian flood basalt sequence at Norilsk, considered to be proxies for parent magmas to the Norilsk-Talnakh orebodies. VB = Voisey's Bay. MCR-K includes Keweenaw basalts from the Mid-*

Continent Rift with trace element characteristics matching the mineralised intrusions. Red dashed line indicates an empirical threshold for "fertile" magmas.

3.3 Recognising deposition sites: identifying cumulate rocks

Favourable intrusions for magmatic sulfide deposits are marked by the presence of cumulate rocks: the solid products of fractional crystallisation (Figure 8A). Cumulates are igneous rocks formed by the accumulation of liquidus phases separated from their parent magmas, regardless of the process by which this accumulation occurs. Some cumulates probably form by mechanical accumulation driven by gravity, either by crystal settling or by deposition from gravity flows, while others form by in-situ nucleation and growth (Wager *et al.* 1960; Campbell 1978; Latypov *et al.* 2017; Latypov *et al.* 2020) or a combination of both (Mao *et al.* 2018). The accumulating components in a cumulate rock are referred to as cumulus phases. Magmatic Ni-Cu sulfide deposits exist where one of the cumulus phases is immiscible sulfide liquid, which in most if not all cases is transported as suspended droplets (Robertson *et al.* 2015) and deposited mechanically by processes related to magma flow dynamics (Barnes *et al.* 2016a; Yao *et al.* 2020; Yao and Mungall 2021). The presence of cumulate silicates, particularly cumulus olivine, pyroxene and spinel, is the distal footprint of these deposition sites, so detection of cumulate rocks is an important objective of lithogeochemistry.

Cumulate rocks can form in two distinct settings relevant to prospectivity: closed-system differentiated bodies, 1) where a body of magma is emplaced in a single event and undergoes fractional crystallisation in place; and 2) where cumulates are deposited in a dynamic open system such as a feeder conduit, with continuous flux and replenishment (Figure 7). Both situations can arise in large or small intrusions; e.g. closed system differentiation in a large layered intrusion such as Skaergaard (Tegner *et al.* 2009) or Kiglapait (Morse 1996), or open system replenishment in the Bushveld Complex (Cameron 1978) or in small ore hosting conduits such as Jinchuan (Li and Ripley 2011) or Xiarihamu (Song *et al.* 2016b). The open system case is much more favourable for Ni-Cu sulfides. The hallmark of open systems is accumulation of a high proportion of uniform cumulates with a limited range of cumulus mineral compositions, reflecting a steady state balance between crystallisation and recharge.

A third setting, related to the second, is mechanical accumulation of crystals and sulfide liquid from a flowing slurry injected into "dead end" intrusions; such systems are not strictly open, but reflect a population of crystals and droplets that have accumulated from a relatively large volume of magma and are hence homogeneous in composition. Geochemically, these are indistinguishable from open-system conduits. This interpretation has been placed on the Nova-Bollinger deposit (Barnes *et al.* 2022a; Taranovic *et al.* 2022) and (controversially) on the ore-hosting Norilsk-Talnakh intrusions (Krivolutskaya *et al.* 2018; Yao and Mungall 2021).

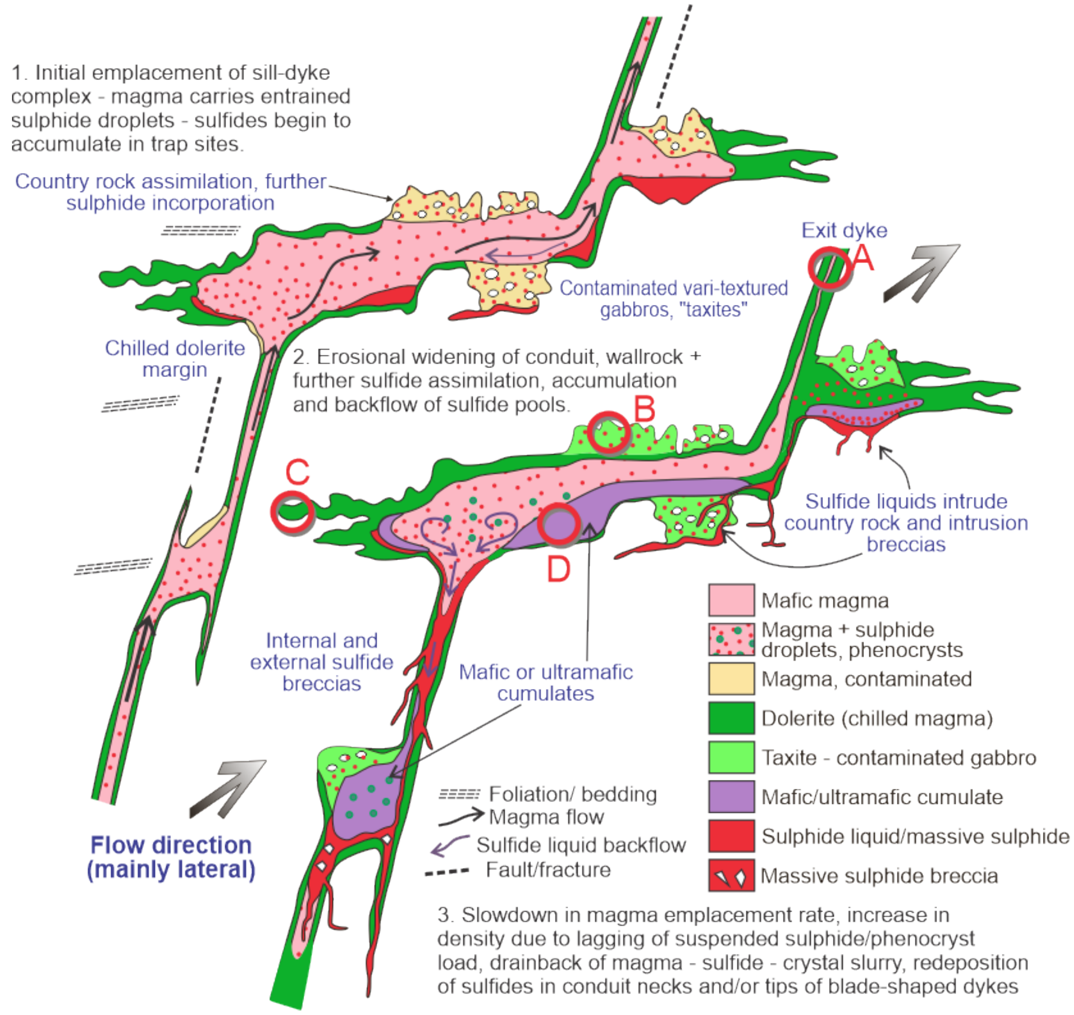

Figure 7. Schematic diagram showing two stages in the development of an intrusion-hosted Ni-Cu-Co sulfide system, modified from Barnes et al. (2016). Ore deposition takes place within part of a larger sill-dyke network with multi-stage assimilation, transport and deposition (Stage 1), re-entrainment and backflow of sulfide liquid droplets and pools (Stage 2) and final deposition during drain-back at the waning stages of magmatism (Stage 3). Geochemical anomalies indicative of ore formation can be present in several components of the system. A) "exit dyke" sampling silicate melt, potentially depleted or enriched in chalcophile elements; B) contaminated marginal taxites with anomalous mineralogy and/or whole rock chemistry; C) distal margins of offshoot dykes and sills preserving early-stage emplacement and transported sulfide droplets; D) cumulate rocks in deposition sites extending beyond sulfide ores – anomalous mineral chemistry and zoning.

The great majority of the known deposits in small mafic-ultramafic intrusions are associated with cumulus olivine, by itself or with cumulus pyroxene. Orthopyroxene (usually bronzite) is the predominant cumulus pyroxene, and is in some cases the dominant phase, e.g at Ntaka Hill (Barnes *et al.* 2016b; Barnes *et al.* 2019a), such that harzburgite or olivine orthopyroxenite are probably the most common host rocks in small intrusions. Kevitsa (Luolavirta *et al.* 2017) and the deposits of the Pechenga belt (Hanski *et al.* 2011) are unusual examples of deposits associated with olivine-clinopyroxene cumulates (wehrlites) with minor orthopyroxene. Pyroxenes in ore-related conduit intrusions tend to have complex trace element zoning patterns (Schoneveld *et al.* 2020b). In more evolved systems plagioclase is also a cumulus phases, and several important deposits have cumulus assemblages of olivine – orthopyroxene-clinopyroxene-plagioclase (olivine gabbronorite) or olivine-clinopyroxene-plagioclase (olivine gabbro) as the dominant lithology; the major example of the latter is Voisey's Bay (Naldrett *et al.* 1996a; Li and Naldrett 1999). Olivine and olivine-plagioclase cumulates are a major component of the host sills to the Norilsk-Talnakh orebodies (Czamanske *et al.* 1995; Barnes *et al.* 2019b). Chromian spinel, usually chromite, is a very widespread accessory phase in most ore-related ultramafic cumulates, particularly olivine-rich ones, but tends to disappear when pyroxene becomes a cumulus phase. Hence, identification of olivine-chromite+/-orthopyroxene cumulates is an important objective for lithogeochemical exploration.

Whole rock compositions of cumulates are determined by the identity and proportion of the cumulus phases and the proportion of parent liquid trapped between the cumulus grains. This can vary from almost zero in adcumulates to as much as 60% in orthocumulates. Small changes in liquid composition close to phase boundaries can generate large discontinuous changes in the mineralogy and whole-rock composition of cumulates, as illustrated in Figure 8. Such changes can be exploited in the recognition of cumulus rocks in geochemical databases.

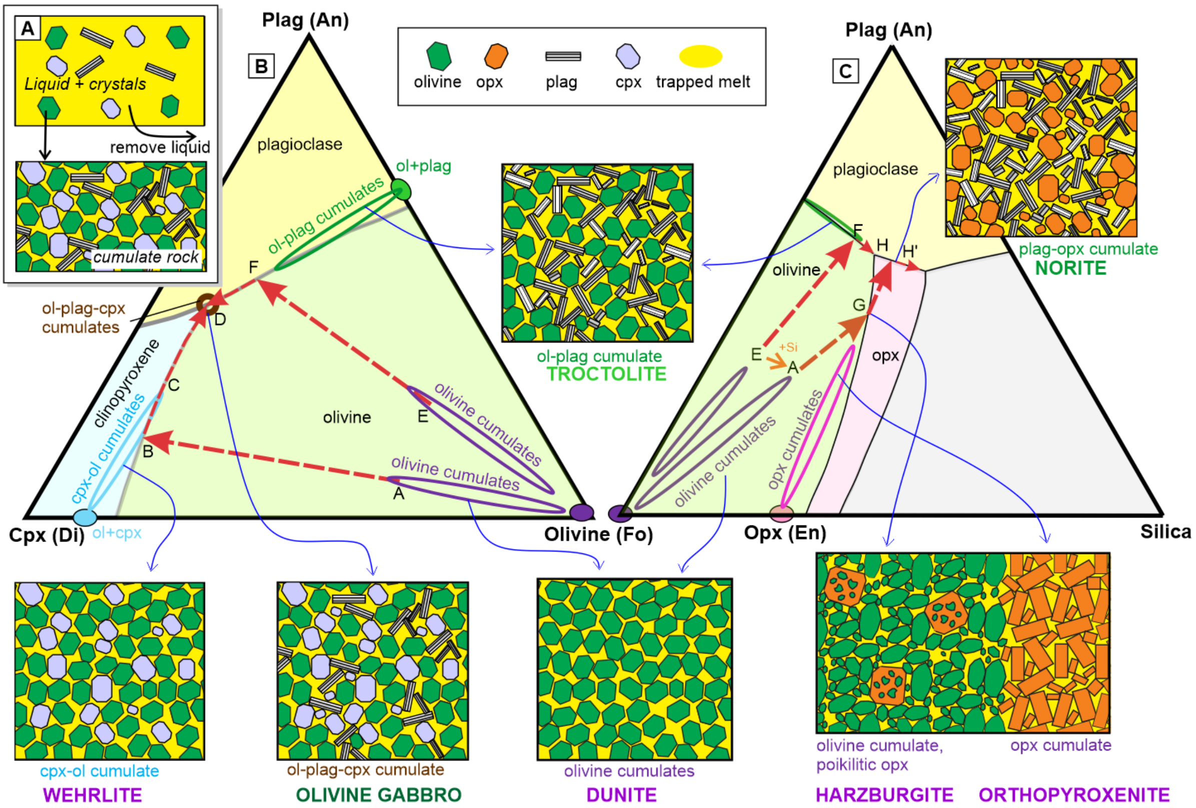

Figure 8. Phase diagrams showing crystallisation sequences of basaltic liquids in the simplified "basalt tetrahedron" system olivine (forsterite) – clinopyroxene (cpx – diopside) – plagioclase (anorthite) – silica. Coloured fields indicate the first phase to crystallise, red dashed line indicate the down-temperature path of evolution of the liquid during perfect fractional crystallisation (crystals removed from the liquid as they form – inset A). Cumulate fields indicate the compositions of the rocks formed as mixtures of cumulus crystals and their parent liquids. For example in the Fo-Di-An projection(B), liquid A crystallises olivine, evolves to point B, crystallises olivine+cpx along path B-C,D. At D, plagioclase begins to crystallise giving rise to an olivine gabbro, olivine+cpx+plag. Liquid E follows a path E-F-D giving olivine, olivine + plagioclase (troctolite), olivine gabbro. If liquid A crystallises to a solid of its own composition, it will produce a non-cumulate rock made mostly of olivine, pyroxene and plagioclase. In the Fo-An-Silica projection (C), crystallisation is complicated by a

"peritectic" phase boundary where olivine reacts with the liquid to form orthopyroxene – path A-G-H-H' giving rise to distinctive poikilitic harzburgite, and eventually norite.

The main messages from the phase diagram (Figure 8) are these.

1. Ultramafic rocks do not require ultramafic magmas. In fact, most "normal" mantle derived basalts can make ultramafic cumulates, provided that they have not evolved too far from their original (mantle melt) compositions.

2. A very minor change in the chemistry of the magma can cause a big jump in the cumulate rock it produces, e.g. from a peridotite (ultramafic - olivine+pyroxene) to a troctolite or a olivine gabbro (mafic). These jumps are commonly present as sharply-bounded layers in ore-hosting intrusions (Latypov *et al.* 2020).

3. A small change in the "starting composition" can cause a big change in crystallisation sequence: e.g. changing the starting composition from A to E in Fig 2C by a small addition of SiO_2 causes the crystallisation path to change from dunite-troctolite-norite along the path E-F-H-H' to dunite-harzburgite-orthopyroxenite-norite along path A-G-H'. The harzburgites formed this way have a characteristic texture called "poikilitic" where large grains of orthopyroxene enclose many smaller, partially dissolved crystal of olivine. This is probably the most widespread rock type associated with intrusion-hosted Ni-Cu-Co deposits.

4. The further down the crystallisation path, the more the solid cumulate product chemically resembles the magma it crystallises from and the harder the cumulate is to recognise.

One or two phase ultramafic cumulates (neglecting chromite) are generally easy to identify from geochemical data in that they form linear arrays on standard binary geochemical plots. However, as magmas become more evolved, the cumulates become harder to recognise (point 4 above). In the idealised phase diagram in Figure 8, they are identical at the ternary eutectic point E. In natural multicomponent systems they continue to evolve with the addition of further cumulus phases such as magnetite, ilmenite and in extreme cases apatite, but will still have the same broadly mafic mineralogy as the products of isochemical solidification of the starting magma. Practically this means that plagioclase-bearing cumulates, i.e. gabbronorites and olivine gabbros, can be difficult to distinguish on their major element chemistry from non-cumulate mafic rocks representing solidified liquids. This can be resolved by the use of two approaches: plots using whole rock Mg number (Mg#, molar percent MgO/[MgO+FeO]) (Figure 9), and molar ratio variation diagrams.

Figure 9 shows a way to distinguish a cumulate gabbro (indicating a deposition site – position 4 in Figure 8) from a mineralogically similar rock that simply represents the magma crystallising to a solid of the same composition – such as might be found in a chilled margin, for example (position 3, Figure 8). Using whole rock data, a plot of Al_2O_3 wt % versus Mg number discriminates cumulate from non-cumulate rocks, because cumulates have higher Mg#, due to Fe-Mg minerals always having higher Mg# than the magmas they crystallise from. Ultramafic cumulates have high Mg# and low Al_2O_3 and plot along curved mixing lines representing mixtures of olivine (or pyroxene, or both) with trapped liquid. Gabbroic cumulates also have high Mg#, although typically slightly lower than ultramafic cumulates because they tend to crystallise from more evolved liquids as is evident from the phase diagram model, but they have much higher Al_2O_3 because of the presence of cumulus plagioclase (vertical vector on Figure 9C)

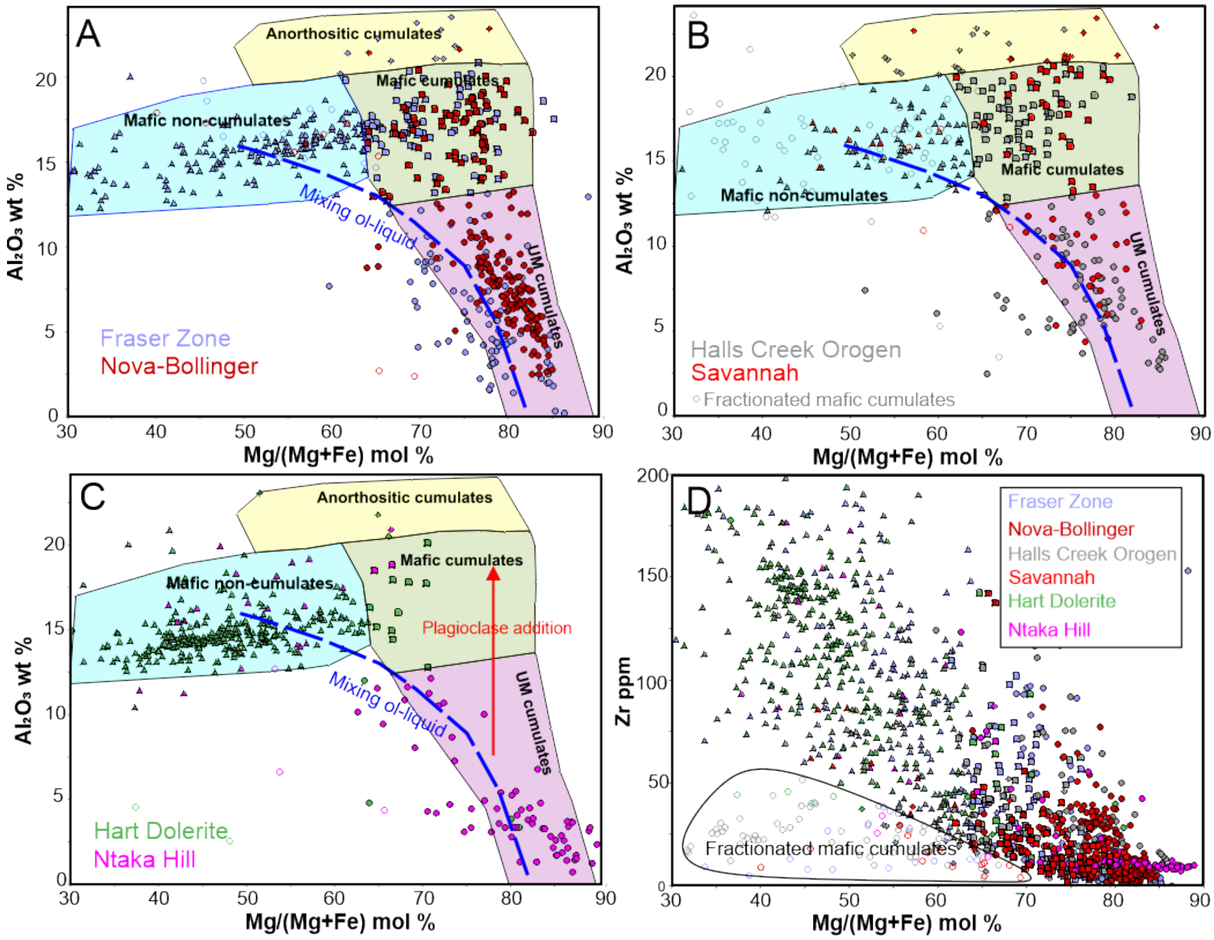

Figure 9. Discriminant plot for ultramafic (UM) and mafic cumulates and non-cumulate mafic rocks. Whole rock data, Al_2O_3 w % versus Mg number (Mg#, molar percent MgO/[MgO+FeO]). Cumulate rocks have higher Mg# due to Fe-Mg minerals always having higher Mg# than the magmas they crystallise from. Individual plots show data for (A) the Fraser Zone of the Albany-Fraser orogen, comparing regional mafic rocks with the host intrusion to the Nova deposit; (B) Halls Creek orogen data compare regional mafic-ultramafic intrusions with the Savannah deposit host intrusion; and (C) the Hart Dolerite is an extensive unmineralised suite of dolerite sills in the Kimberley Craton, showing an almost complete absence of ultramafic cumulates and the Ntaka Hill deposit, hosted by an almost entirely ultramafic host body containing an abundance of orthopyroxene cumulates. (D) Plot of whole rock Zr vs Mg number, showing field for mafic cumulates derived from strongly fractionated Fe-rich mafic parent magmas. See table 1 for data sources, and table 2 for formulae for calculation of molar values).

Not all ore-hosting intrusions contain ultramafic cumulates, where the cumulus phases are combinations of olivine, pyroxene and (usually) minor chromite, but there are very few that don't. As can be seen in Figure 9, the ore-bearing intrusions in a number of prospective belts are strongly dominated by cumulate rocks compared with other mafic rocks in the same belt, a particularly clear example being the Nova intrusions in the Fraser Zone of Albany Fraser orogen. The Hart Dolerite represents a very high-volume Large Igneous Province almost completely devoid of cumulate rocks that has so far proved entirely barren for this deposit type. This would be typical of the signatures of unmineralized suites of mafic rocks.

There are two important caveats in the use of the Al_2O_3 w % versus Mg number plot. Firstly, in closed-system intrusions, such as the Skaergaard intrusion or differentiated dolerite sills like the Golden Mile Dolerite at Kalgoorlie, the Mg number of the cumulus phases can evolve to very low values – almost to zero in the Skaergaard case, where almost complete fractional crystallisation took place (Nielsen *et al.* 2015). Such rocks would plot in the "non-cumulate" field of the Al_2O_3 versus Mg number plot. These can be discriminated by plotting highly incompatible element, such as Zr, against Mg# as in Figure 9D. Such elements are at much lower concentrations in cumulates than the parent liquid for the same Mg#, due to the presence of the (e.g.) Zr-free cumulus phases. Where this approach is used, the Zr-Mg# plot should be used first to filter for this category. The second caveat concerns komatiites, where non-cumulate komatiitic liquids can plot at high Mg#; these diagrams are designed for use in provinces dominated by mafic magmas.

An alternative to the Al_2O_3 w % versus Mg number plot uses the mass ratio Al_2O_3 / TiO_2 versus Mg number. An example is shown in Figure 10. Mixing of ultramafic cumulus assemblages of olivine and/or pyroxene with liquid generates an approximately horizontal trend, because the Al and Ti contents of the solid phases are low. Addition of cumulus plagioclase causes a rapid increase in Al_2O_3/TiO_2 generating the L-shaped trends shown. This plot is complicated by the effect of the liquid component becoming progressively enriched with Ti over Al as fractionation proceeds, up to the point of magnetite saturation, and also by the presence of high Al in cumulus pyroxenes in high pressure cumulates such as those at Nova-Bollinger, but is nevertheless useful in discriminating relatively primitive ultramafic and mafic cumulate rocks. The same caveats apply as for Al_2O_3 versus Mg number.

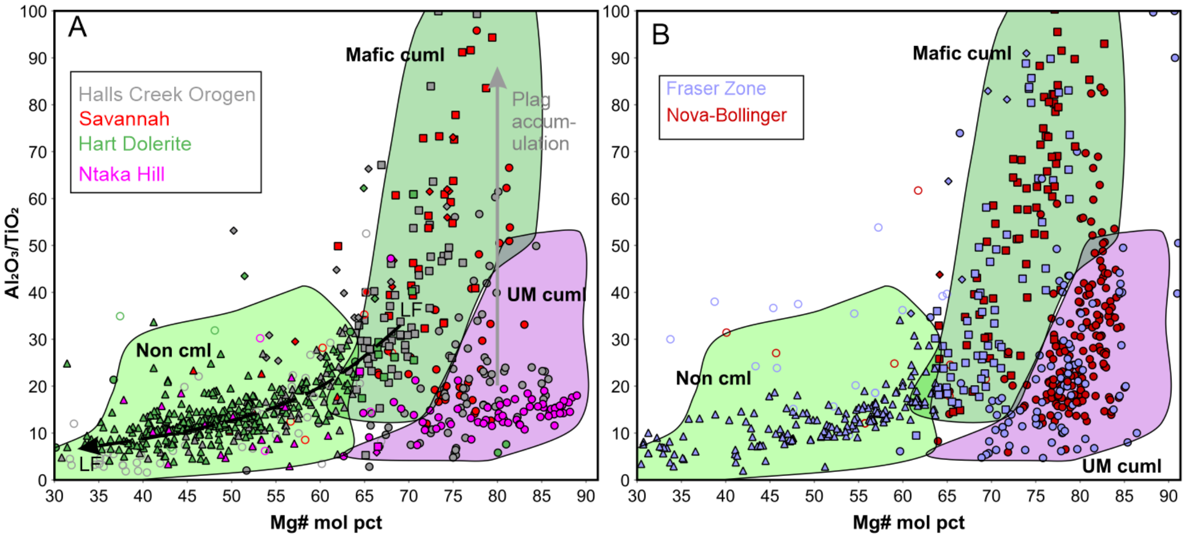

Figure 10 Al_2O_3 / TiO_2 versus Mg number plot for discrimination ultramafic and mafic cumulates (UM cuml, Mafic cuml) from mafic non-cumulates. Data from Halls Creek Orogen, Fraser Zone, Ntaka Hill. Dashed line labelled LF indicates path taken by fractional; crystallisation of a plagioclase-saturated liquid.

Recognising ultramafic cumulate rocks is generally fairly straightforward: they are high in Mg, Cr and Ni and low in components such as Al and Ti that are not concentrated in these minerals. However, ultramafic rocks are very susceptible to alteration, which can modify their chemistry, and weathering, which is discussed below. Orthopyroxene is a particularly useful indicator, in that most mantle-derived magmas don't crystallise much of it. The presence of orthopyroxene cumulates is a good indication that magmas have been contaminated with silica-rich country rocks (causing the shift from composition E to A in Figure 8C), which is another positive indicator for fertility.

Figure 11 shows a geochemical technique that allows the recognition of olivine and orthopyroxene cumulates from whole-rock geochemistry, to be used in conjunction with Figure 9 and Figure 10. It is important to note that this method requires reliable SiO_2 analyses, which are not provided in some element suites such as the standard ICP-OES package offered by many commercial laboratories. Silica is such an important component that it is generally worth the additional cost to analyze it using the more comprehensive ICP-MS method, even if that is at the expense of dropping off some of the lower-abundance trace elements like Se, Te and Bi that are typically below the limit of detection in cumulate rocks. The mineralised Ntaka Hill intrusion in Tanzania (Barnes *et al.* 2019) shows up clearly as an intrusion with abundant orthopyroxene cumulates (Fig. 4).

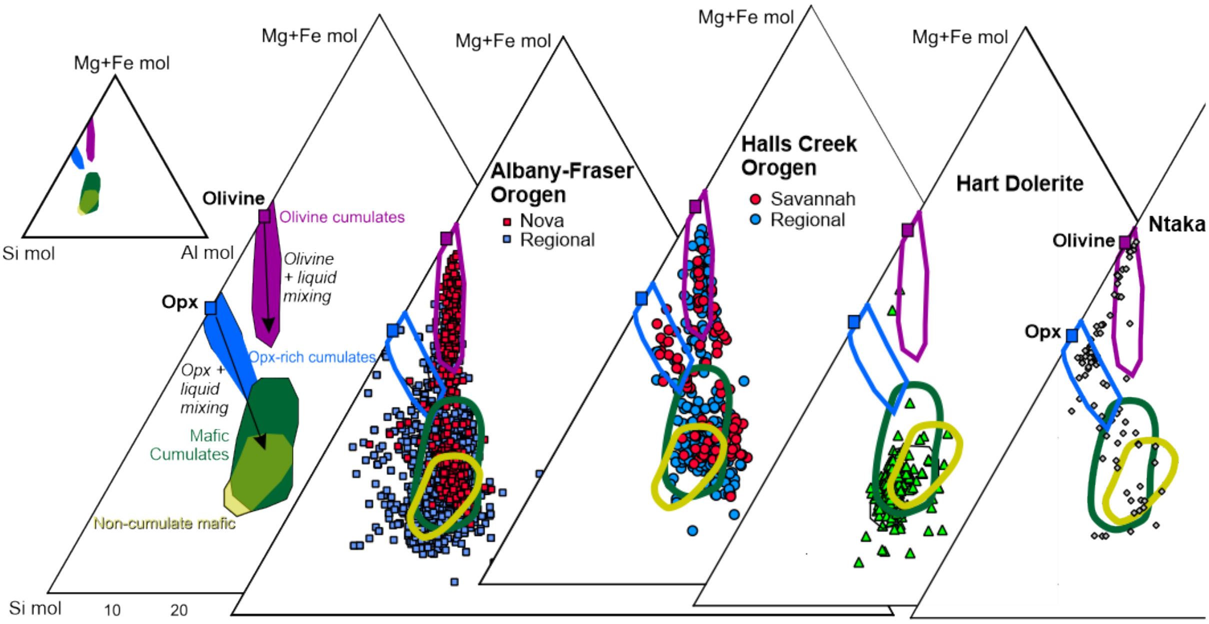

Figure 11. Triangular plot – molar ratio of MgO + FeO, SiO_2 and Al_2O_3 (see Table 1 for the calculation method) for discrimination of olivine and orthopyroxene (opx) dominated cumulates from cumulate and non-cumulate gabbros. Same data sets as Figure 3.

A further example of this approach, and the Al/Ti vs Mg# plot, is that they are using element ratios that are unaffected by dilution by volatiles (H_2O, CO_2) during alteration. In the case of ultramafic rocks alteration can be accompanied by introduction of up to 20% of these components, causing reduction of major element oxides due to closure (analyses must sum to 100%). Use of element ratios and triangular plots (effectively ratio plots) mitigates this effect.

4 Detecting ore-forming processes

At a prospect scale, the focus moves from target selection to vectoring towards ore and eventually (hopefully) to orebody definition. Geochemical proxies are used at this scale to identify the distal signals of ore forming processes. Within prospective intrusions, mapping out ultramafic and gabbroic cumulates from non-cumulate chilled liquid rocks using spatially constrained geochemical datasets, as described above, provides a powerful tool for unravelling the internal structure of a potentially fertile magmatic system. More obviously, recognising subtle signals of sulfide deposition and fractional extraction can potentially serve as direct vectoring tools.

4.1 Ni in olivine and whole rock

Nickel contents of olivine have been widely used as petrogenetic indicators and as fertility indicators for magmatic sulfide potential of mafic-ultramafic intrusions, mainly predicated on the assumption that olivines crystallized from magmas that had equilibrated with sulfide liquid should be relatively depleted in Ni compared with sulfide-free baseline. This has given rise to a large accumulation of data on volcanic and intrusive rocks. Results are discussed in detail by Barnes et al. (2021b) and a brief summary follows.

Ni content of olivine, at given Fo content, is subject to wide range of controls, not all of which can be attributed to sulfide interaction. Baselines for Ni in olivine in relation to Fo content are somewhat lower in orogenic belt settings relative to intrusions in continental LIPs. No clear, universal discrimination is evident in Ni in olivine between ore-bearing, weakly mineralized and barren intrusions even when tectonic setting is taken into account. However, sulfide-related signals can be picked up at intrusion scale in many cases. Low-R factor, low-tenor sulfides are associated with low-Ni olivines in a number of examples such as Kabanga (Maier *et al.* 2011) and these cases stand out clearly. Anomalously high-Ni olivines are a feature of some mineralized intrusions. In these cases, enrichment may be due to crystallisation of trapped liquid in orthocumulates or re-entrainment of "primitive" Ni-rich sulfide by a more evolved Fe-rich magma, driving the olivine to become Ni-enriched due to Fe-Ni exchange reaction between sulfide and olivine. Wide variability of both Fo and Ni within and between related intrusions at regional scale may be a useful prospectivity indicator. In general, the use of Ni-olivine as a fertility tool is more likely to generate false negatives than false positives, but both are possible.

Nickel in olivine is an important control on whole-rock Ni contents of sulfide-free cumulate rocks, but in many cases the whole rock Ni signal is overwhelmed by the variation in the modal proportions of the different cumulus phases in the rock (Figure 12). This is important for establishing baseline levels of silicate Ni in unmineralized rocks and hence for recognising the presence of minor components of sulfide. Because of the uncertainties involved, Ni background levels in multi-phase cumulates are unpredictable (Figure 12), such that it is generally more reliable to use the Cu content rather than the Ni content as a proxy for presence of minor traces of magmatic sulfide. This will apply as long as the rocks are not excessively altered such that Cu may be mobile.

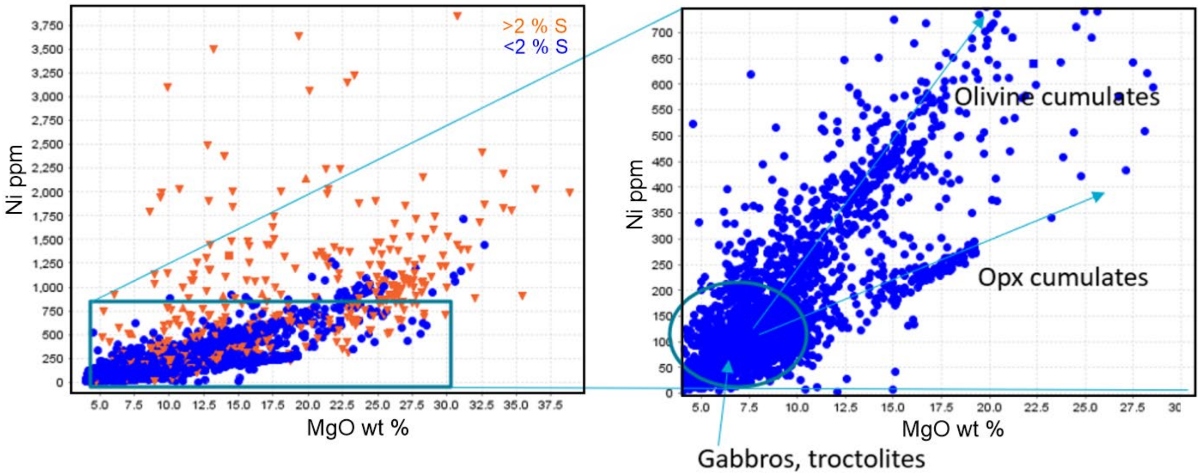

Figure 12 Ni vs MgO in mineralised vs barren cumulate rocks in Proterozoic orogenic belts. Blue indicates samples with <0.5% S, orange >0.5%. Note that there is considerable overlap, attributable to the variability in S-free background due to variability in cumulus mineralogy.

4.2 Detecting trace sulfides: Cu and Cu/Zr ratios in fresh cumulate rocks

Copper behaves as an incompatible element during crystallisation of cumulus silicate minerals from a sulfide-undersaturated magma, such that the ratio of Cu to other incompatible elements such as Zr remains constant. Furthermore, it retains the value in the original magma and indeed in the original mantle source (assuming no sulfide was left in the mantle restite). Extraction of a cumulus sulfide component causes Cu to be depleted relative to Zr due to the strongly chalcophile character of Cu (Kiseeva and Wood 2015), such that this ratio can be used as a proxy for ore forming processes (Maier *et al.* 1998). Values of Cu/Zr significantly lower than the expected primitive mantle (PM) value of ~5 (McDonough and Sun 1995) are potentially indicative of magmas that have experienced fractional extraction of sulfide liquid. Conversely, rocks that contain even a small component of accumulated sulfide liquid should have Cu/Zr greater than the PM value.

This principle is tested using three extensive data sets, the Fraser Zone, the Halls Creek Orogen (Table 1) and the Hart Dolerites (Figure 13)

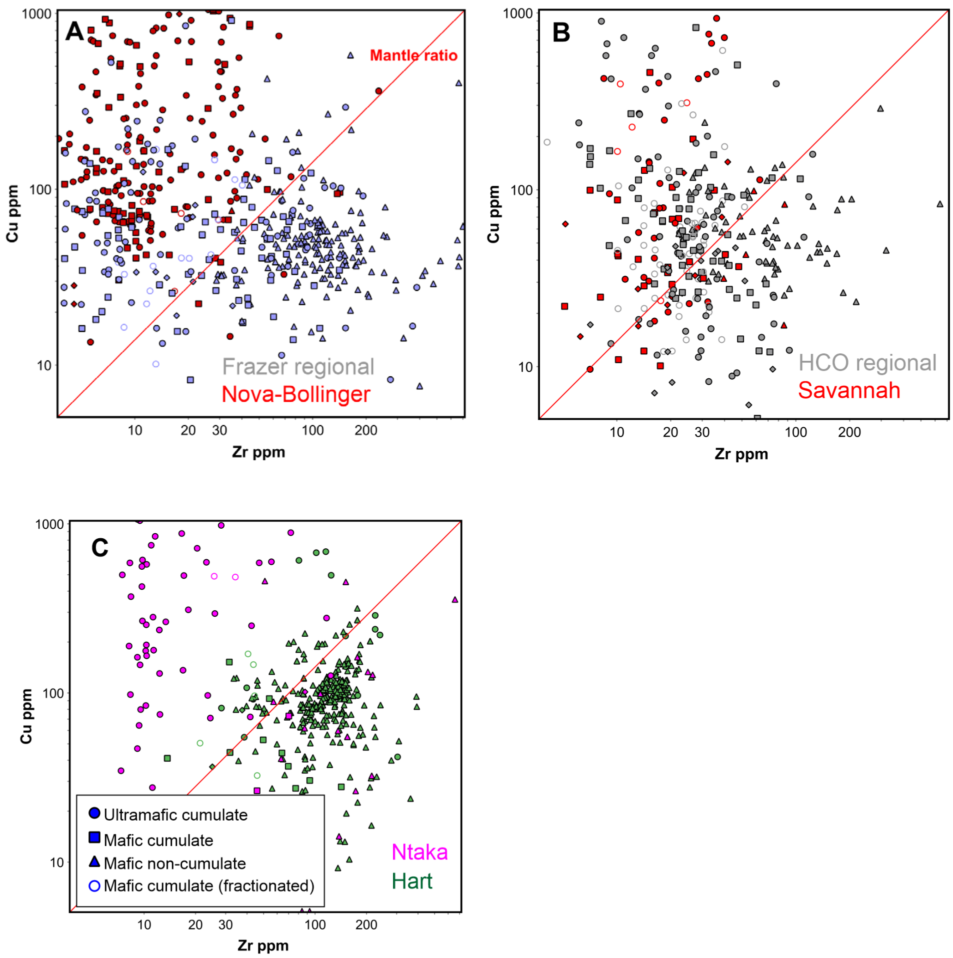

Figure 13. Zr vs Cu for selected data sets (Table 1). A, Fraser Zone gabbros and dolerite "background" compared with samples from the Nova – Bollinger intrusions. B, Savannah intrusions compared with "background" from the Halls Creek Orogen, and samples from the entirely unmineralized Hard Dolerite.

The Fraser Zone data shows a very clear distinction between the mineralized Nova-Bollinger complex and the "background" Fraser Gabbros and other intrusions and meta-dolerites. Presence of cumulus sulfides is clearly defined by Cu/Zr values on the Cu-rich side of the mantle line while the background grouping straddles the line and shows a strong mode with high Zr and distinctly depleted Cu. These compositions are plausibly interpreted as magmas that fractionated sulfide liquid, some of which may have been picked up and transported into the orebodies. A similar although less well-defined pattern is observed in the Halls Creek dataset, although here the mineralised samples appear to contain both Cu-enriched and depleted components. The mainly unmineralized background straddles the mantle line and extends to distinctly Cu depleted compositions. The Hart Dolerite set is strongly clustered on the Cu-depleted side of the mantle line with no samples indicating Cu enrichment. The apparent depletion in this case is so consistent that it probably represents a source characteristic, i.e. the assumption of a mantle source with Cu/Zr = 5 is not correct. More significant is the fact that the unmineralized suite has a consistent, tightly clustered distribution with no enrichment, in contrast to the mineralized belts showing a wide spread of both depleted and enriched samples.

The benefit of the Cu-Zr approach is that these elements are quite commonly available in regional pre-competitive datasets such as geological survey databases. They are therefore amenable to data mining in a way that other potential discriminants such as PGEs are not. The potential drawback is the high mobility of Cu during hydrothermal alteration, such that the approach is only reliable where the rocks are for the most part reasonably pristine.

4.3 Detecting contamination using variably incompatible lithophile elements

A key component of the standard genetic model is that ore-forming magmas need to interact with the country rocks in order to assimilate sulfide (or sulfate) and this process should lead to distinct signals of crustal contamination. This approach has been widely applied to komatiitic systems, where it appears to be useful as a belt-scale discriminant but not so much on a local scale, due to the complexities of flushed and recharged magma channels (Lesher *et al.* 2001; Barnes *et al.* 2007; Barnes and Fiorentini 2012; Barnes *et al.* 2013) and the effects of variable time-scales for component processes in ore formation (Barnes and Robertson 2019). However, the approach has generally proved less successful in mafic-hosted systems.

We have already seen geochemical effects of contamination in the Th/Yb vs Nb/Yb plots (Figure 2, Figure 3). Mineralized intrusions tend to follow the crustal contamination trend of steeply increasing Th/Yb over limited Nb/Yb, which follows from the high abundance of Th relative to Nb and Yb in most crustal rocks. This trend is essentially the same as that seen in Archean komatiite-basalt sequences. However, within individual provinces such as FZ and HCO, there is no particular preference for crustal contamination trends to be present in the ore-bearing intrusions as opposed to the regional unmineralized or weakly mineralized intrusions. It is likely that crustal contamination is so widespread in continental settings that proxies for it generate far too many false positives to be useful at the scale of individual intrusions.

4.4 Use of preserved element ratios

When interpreting lithogeochemical data on highly altered or moderately weathered rocks, it is important to recognise that some otherwise informative elements such as Mg, Si, S and Cu might be highly mobile and hence useless. A solution to this problem is to use ratios of relatively immobile elements whose relative proportions are insensitive to alteration and mild to moderate degrees of weathering. This category includes such useful elements as Ni, Cr, Ti, Zr and the REE, and use of rations between these elements has been applied to mapping of variably weathered komatiites and basalts in lateritic terranes. (Barnes *et al.* 2014). Triangular plots of combinations of these elements are particularly reliable and informative (Figure 14).

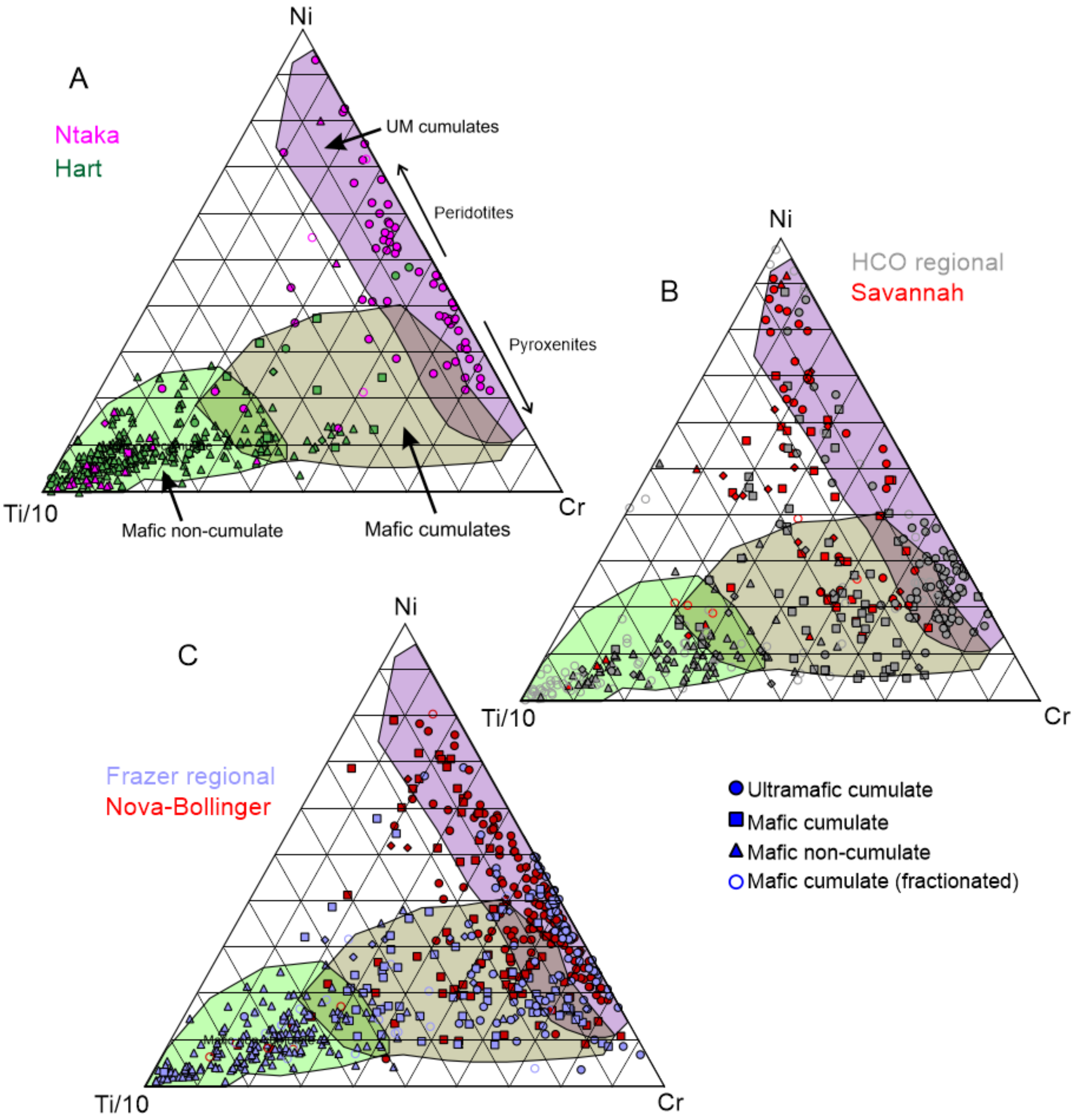

Figure 14. Ni-Cr-Ti plots showing discrimination of cumulate rock types and sulfide bearing samples using retained trace element ratios. S-poor samples (<0.7 % S) only. Colour indicates locality, shape indicates rocktype. This approach is applicable to moderately weathered and altered rocks, and hence can be applied to top-of-fresh-rock sampling in weathered terranes.

5 Concluding remarks

The primary purpose of this contribution is to de-mystify some of the principles of igneous petrology that underpin geochemical variability, and to translate those into easily usable proxies that can add value to large bodies of data acquired during exploration programs. Some of the plots shown here are also applicable to data-mining legacy datasets.

Based on an extensive data compilation, exemplified by the regional datasets we have presented here, there are a number of distinct proxies which, when taken together, can be used to prioritise targets, if not to specifically zero in on targets.

1. Mineralised terrains tend to have incompatible trace element patterns indicative of mixing of magmas from primitive or mildly deleted mantle sources with an overprint of contamination by continental crust. These can be identified on plots of Th/Nb vs Nb/Yb.
2. Mineralised intrusions in almost all cases contain cumulate rocks, with a strong preponderance of olivine-bearing cumulates. Orthopyroxene cumulates are favourable indicators in some terranes but are not universally present. These can be identified using a number of different plots involving whole rock analyses of Mg, Fe, Al and Zr, and triangular plots using whole-rock Ni, Cr and Ti.
3. Terrains where mafic intrusions are dominated by non-cumulate rocks tend to have low prospectivity.
4. Indicators of high-Mg magmas such as high Fo contents in olivine do not appear to have useful predictive value.
5. Chalcophile element enrichments and depletions at terrane and intrusion scale are positive indicators, with Cu vs Zr being a useful discriminant in all but highly altered rocks. Platinum group elements are of limited use owing to the very wide variability in parent magmas.
6. In addition, the presence of widely variable Ni content in olivine and pyroxene for similar forsterite content in olivine is a strong positive indicator but requires high-precision microprobe analyses.

It is important to emphasize that these approaches should be combined with all other available datasets in a weigh-of-evidence approach. There are no geochemical silver bullets. Importantly, geochemical datasets are self-evidently only applicable to the rocks that were sampled. In many potential target terranes, there is no guarantee that unsampled rocks may show positive indicators. For example, the mineralized cumulate-bearing intrusions at Norilsk-Talnakh account for only about one part per million of the total volume of the Siberian Large Igneous Province (Barnes *et al.* 2020). That said, it is hoped that the tools and techniques presented here will allow explorers to apply geochemical proxies for ore-forming processes, improve rock type identification and in other ways add value to the large volumes of geochemical data that already exist and continue to be collected.

Table 2. Data sources for figures.

Locality	Belt	Craton/region	Reference

Eagle	Mid-Continent Rift USA	Mid-Continent	(Ding *et al.* 2010; Ripley and Li 2011)
Emeishan	Emeishan	Yangtze Craton	(Song *et al.* 2006; Tao *et al.* 2008; Hanski *et al.* 2010; Pang *et al.* 2010; Li *et al.* 2012a)
Hart Dolerite	Kimberley Craton LIP	Kimberley Craton LIP	Geological Survey of WA WACHEM database https://www.dmp.wa.gov.au/GeoChem-Extract-Geochemistry-1559.aspx
Huangshandong	Tianshan nickel belt	Central Asian Orogenic Belt	(Gao *et al.* 2013) (Mao *et al.* 2015) (Sun *et al.* 2013) (Mao *et al.* 2014) (Zhao *et al.* 2016)
Huangshannan	Tianshan nickel belt	Central Asian Orogenic Belt	(Zhao *et al.* 2016)
Huangshanxi	Tianshan nickel belt	Central Asian Orogenic Belt	(Mao *et al.* 2014)
Jinchuan	Longshoushan	North China	(Chai and Naldrett 1994; Li *et al.* 2005; Li and Ripley 2011)
Kalatongke	East Tianshan nickel belt		(Li *et al.* 2012b; Mao *et al.* 2022) (Zhang *et al.* 2009; Gao and Zhou 2013; Tang *et al.* 2020)
Norilsk-Talnakh deposits	Siberian Traps	Siberian Craton	(Barnes and Kunilov 2000; Li *et al.* 2003; Barnes *et al.* 2019b; Schoneveld *et al.* 2020a; Krivolutskaya *et al.* 2021)
Kalgoorlie Terrane	East Yilgarn nicke province (komatiitic)	Eastern Goldfields Superterrane, Yilgarn Craton	(Barnes *et al.* 2021a)
Nova-Bollinger	Albany-Fraser	Yilgarn Craton unspecified	(Maier *et al.* 2016; Taranovic *et al.* 2022)
Ntaka Hill	Mozambique Mobile Belt	East African Shield	(Barnes *et al.* 2016b; Mole *et al.* 2017; Barnes *et al.* 2019a)
Pechenga	Pechenga	Baltic Shield, NW Russia	(Hanski and Smolkin 1989; Hanski 1992; Hanski *et al.* 2011)
Savannah	Halls Creek Orogen	North Australian Craton	(Mole *et al.* 2018; Le Vaillant *et al.* 2020)
Siberian Traps basalts	Siberian Traps	Siberian Craton	(Lightfoot *et al.* 1990; Brugmann *et al.* 1993; Lightfoot and Keays 2005)
Tamarack	MidContinent Rift USA	Mid-Continent	(Taranovic *et al.* 2015)
Voisey's Bay	Nain Plutonic Province		(Li and Naldrett 1999)
Xiarihamu	East Kunlun Orogenic Belt	Tibet	(Li *et al.* 2015b; Song *et al.* 2016b; Song *et al.* 2020)

Table 2.

Factors for calculating molar components in discriminant plots.

Mg mol	MgO/40.3
Fe mol	[Total Fe as FeO*]/71.9
Si mol	SiO_2/60.1
Al mol	Al_2O_3/51
Mg#	100 x Mg mol/[Mg mol + Fe mol]

*See supplementary appendix 1 for splitting of whole rock FeO, Fe_2O_3 and sulfide-associated Fe. The approximation potentially introduces a small error, up to about relative 3%, in cumulate rocks.

6 Acknowledgments

7 References

Arndt, N. 2013. The lithospheric mantle plays no active role in the formation of orthomagmatic ore deposits. *Economic geology and the Bulletin Of the Society Of Economic Geologists*, **108**, 1953-1970, https://doi.org/https://doi.org/10.2113/econgeo.108.8.1953.

Arndt, N.T. 2011. Insights into the Geologic Setting and Origin of Ni-Cu-PGE Sulfide Deposits of the Norilsk-Talnakh Region, Siberia. *Reviews in Economic Geology*, **17**, 199-215.

Barnes, S.-J. and Lightfoot, P.C. 2005. Formation of magmatic nickel sulfide deposits and processes affecting their copper and platinum group element contents. *Economic Geology 100th Anniversary Volume*, 179-214.

Barnes, S.J. 2006. Komatiite-hosted nickel sulfide deposits: geology, geochemistry, and genesis. *Society of Economic Geologists Special Publication*, **13**, 51-118.

Barnes, S.J. and Kunilov, V.Y. 2000. Chrome Spinels and Mg-ilmenites from the Noril'sk 1 and Talnakh intrusions and other mafic rocks of the Siberian flood basalt province. *Economic Geology*, **95**, 1701-1717.

Barnes, S.J. and Fiorentini, M.L. 2012. Komatiite magmas and nickel sulfide deposits: a comparison of variably endowed Archean terranes. *Economic Geology*, **107**, 755-780, https://doi.org/10.2113/econgeo.107.5.755.

Barnes, S.J. and Mungall, J.E. 2018. Blade shaped dykes and nickel sulfide deposits: a model for the emplacement of ore-bearing small intrusions. *Economic Geology*, **113**, 789-798, https://doi.org/10.5382/econgeo.2018.4571.

Barnes, S.J. and Robertson, J.C. 2019. Time scales and length scales in magma flow pathways and the origin of magmatic Ni-Cu-PGE ore deposits. *Geoscience Frontiers*, **10**, 77-87, https://doi.org/https://doi.org/10.1016/j.gsf.2018.02.006.

Barnes, S.J., Lesher, C.M. and Sproule, R.A. 2007. Geochemistry of komatiites in the Eastern Goldfields Superterrane, Western Australia and the Abitibi Greenstone Belt, Canada, and implications for the distribution of associated Ni-Cu-PGE deposits. *Applied Earth Science (Transactions of the Institute of Mining and Metallurgy Series B)*, **116**, 167-187.

Barnes, S.J., Heggie, G.J. and Fiorentini, M.L. 2013. Spatial variation in platinum group element concentrations in ore-bearing komatiite at the Long-Victor deposit, Kambalda Dome, Western Australia: enlarging the footprint of nickel sulfide orebodies. *Economic Geology*, **108**, 913-933, https://doi.org/10.2113/econgeo.108.5.913.

Barnes, S.J., Mungall, J.E. and Maier, W.D. 2015. Platinum group elements in mantle melts and mantle samples. *Lithos*, **232**, 395-417, https://doi.org/10.1016/j.lithos.2015.07.007.

Barnes, S.J., Holwell, D.A. and Le Vaillant, M. 2017a. Magmatic sulfide ore deposits. *Elements*, **13**, 91-97, https://doi.org/10.2113/gselements.13.2.91

Barnes, S.J., Malitch, K.N. and Yudovskaya, M.A. 2020. Introduction to a Special Issue on the Norilsk-Talnakh Ni-Cu-Platinum Group Element Deposits. *Economic Geology*, **115**, 1157-1172, https://doi.org/10.5382/econgeo.4750.

Barnes, S.J., Stanley, C.R. and Taranovic, V. 2022a. Compositions and Ni-Cu-PGE tenors of Nova-Bollinger ores with implications for the origin of Pt anomalies in PGE-poor massive sulfides. *Economic Geology*, **online**, https://doi.org/10.5382/econgeo.4894.

Barnes, S.J., Fisher, L.A., Anand, R.R. and Uemoto, T. 2014. Mapping bedrock lithologies through in-situ regolith using retained element ratios: a case study from the Agnew-Lawlers area, Western Australia. *Australian Journal of Earth Sciences*, **61**, 269-285, https://doi.org/10.1080/08120099.2014.862302.

Barnes, S.J., Cruden, A.R., Arndt, N.T. and Saumur, B.M. 2016a. The mineral system approach applied to magmatic Ni-Cu-PGE sulphide deposits. *Ore Geology Reviews*, **76**, 296-316, https://doi.org/10.1016/j.oregeorev.2015.06.012.

Barnes, S.J., Mole, D.R., Hornsey, R. and Schoneveld, L.E. 2019a. Nickel-copper sulfide mineralization in the Ntaka Hill Ultramafic Complex, Nachingwea region, Tanzania. *Economic Geology*, **114**, 1135-1158.

Barnes, S.J., Le Vaillant, M., Godel, B. and Lesher, C.M. 2019b. Droplets and bubbles: solidification of sulphide-rich vapour-saturated orthocumulates in the Noril'sk-Talnakh Ni-Cu-PGE ore-bearing intrusions *Journal of Petrology*, **60**, 269-300, https://doi.org/10.1093/petrology/egy114.

Barnes, S.J., Staude, S., Le Vaillant, M., Pina, R. and Lightfoot, P.C. 2018. Sulfide-silicate textures in magmatic Ni-Cu-PGE sulfide ore deposits: massive, semi-massive and sulfide-matrix breccia ores. *Ore Geology Reviews*, **101**, 629-651, https://doi.org/10.1016/j.oregeorev.2018.08.011.

Barnes, S.J., Williams, M.J., Smithies, R.H., Lowrey, J.R. and Hanski, E. 2021a. Trace element contents of mantle-derived magmas through time. *Journal of Petrology*, **62**, https://doi.org/10.1093/petrology/egab024.

Barnes, S.J., Osborne, G.A., Cook, D., Barnes, L., Maier, W.D. and Godel, B.M. 2011. The Santa Rita Nickel Sulfide Deposit in the Fazenda Mirabela Intrusion, Bahia, Brazil: geology, sulfide geochemistry and genesis. *Economic Geology*, **106**, 1083-1110.

Barnes, S.J., Mole, D.R., Le Vaillant, M., Campbell, M., Verrall, M., Roberts, M. and Evans, N.J. 2016b. Poikilitic textures, heteradcumulates and zoned orthopyroxenes in the Ntaka Ultramafic Complex, Tanzania: implications for crystallisation mechanisms of oikocrysts. *Journal of Petrology*, **57**, 1171-1198, https://doi.org/10.1093/petrology/egw036.

Barnes, S.J., Yao, Z.-S., Mao, Y.J., Jesus, A.P., Yang, S.H., Taranovic, V. and Maier, W.D. 2022b. Nickel in olivine as an exploration indicator for magmatic Ni-Cu sulfide deposits: a data review and re-evaluation. *AMERICAN MINERALOGIST*, **online**, https://doi.org/10.2138/am-2022-8327.

Barnes, S.J., Mungall, J.E. *et al.* 2017b. Sulfide-silicate textures in magmatic Ni-Cu-PGE sulfide ore deposits: Disseminated and net-textured ores. *AMERICAN MINERALOGIST*, **102**, 473-506, https://doi.org/10.2138/am-2017-5754.

Barnes, S.J., Ryan, C.G. *et al.* 2021b. Spatial association between platinum minerals and magmatic sulfides imaged with the Maia Mapper and implications for the origin of the Chromite-sulfide-PGE association. *Canadian Mineralogist*, **59**, 1775-1799, https://doi.org/10.3749/canmin.2000100.

Begg, G.C., Hronsky, J.A.M., Arndt, N.T., Griffin, W.L., O'Reilly, S.Y. and Hayward, N. 2010. Lithospheric, cratonic and geodynamic setting of Ni-Cu-PGE sulfide deposits. *Economic Geology*, **105**, 1057-1070.

Bennett, M., Gollan, M., Staubmann, M. and Bartlett, J. 2014. Motive, Means, and Opportunity: Key Factors in the Discovery of the Nova-Bollinger Magmatic Nickel-Copper Sulfide Deposits in Western Australia. *Society of Economic Geologists Special Publication*, **18**, 301-320.

Brugmann, G.E., Hanski, E.J., Naldrett, A.J. and Smolkin, V.F. 2000. Sulphide segregation in ferropicrites from the Pechenga Complex, Kola Peninsula, Russia. *Journal of Petrology*, **41**, 1721-1742.

Brugmann, G.E., Naldrett, A.J., Asif, M., Lightfoot, P.C., Gorbachev, N.S. and Fedorenko, V.A. 1993. Siderophile and chalcophile metals as tracers of the evolution of the Siberian Trap in the Noril'sk region, Russia. *Geochimica et Cosmochimica Acta*, **57**, 2001-2018.

Cameron, E.N. 1978. The lower zone of the eastern Bushveld Complex in the Oliphants River Trough. *Journal of Petrology*, **19**, 437-462.

Campbell, I.H. 1978. Some problems with the cumulus theory. *Lithos*, **11**, 311-323.

Campbell, I.H. and Griffiths, R.W. 1990. Implications of mantle plume structure for the evolution of flood basalts. *Earth and Planetary Science Letters*, **99**, 79-93.

Chai, G. and Naldrett, A.J. 1992. The Jinchuan ultramafic intrusion: cumulate of a high-Mg basaltic magma. *Journal of Petrology*, **33**, 277-304.

Chai, G. and Naldrett, A.J. 1994. Pyroxene mineral chemistry of the Jinchuan Intrusion, China. *Mineralogy and Petrology*, **51**, 1-20.

Condie, K. 2015. Changing tectonic settings through time: Indiscriminate use of geochemical discriminant diagrams. *Precambrian Research*, **266**, 587-591, https://doi.org/https://doi.org/10.1016/j.precamres.2015.05.004.

Czamanske, G.K., Zen'ko, K.E. *et al.* 1995. Petrographic and geochemical characterization of ore-bearing intrusions of the Noril'sk Type, Siberia; with discussion of their origin. *Resource Geology Special Issue*, **18**, 1-48.

Ding, X., Li, C., Ripley, E.M., Rossell, D. and Kamo, S. 2010. The Eagle and East Eagle sulfide ore-bearing mafic-ultramafic intrusions in the Midcontinent Rift System, upper Michigan: Geochronology and petrologic evolution. *Geochemistry, Geophysics, Geosystems*, **11**, https://doi.org/https://doi.org/10.1029/2009GC002546.

Fiorentini, M.L., Barnes, S.J., Maier, W.D., Burnham, O.M. and Heggie, G.J. 2011. Global variability in the platinum-group element contents of komatiites. *Journal of Petrology*, **52**, 83-112, https://doi.org/10.1093/petrology/egq074.

Fiorentini, M.L., Barnes, S.J., Lesher, C.M., Heggie, G.J., Keays, R.R. and Burnham, O.M. 2010. Platinum-group element geochemistry of mineralized and non-mineralized komatiites and basalts. *Economic Geology*, **105**, 795-823.

Gao, J. and Zhou, M. 2013. Magma mixing in the genesis of the Kalatongke dioritic intrusion; implications for the tectonic switch from subduction to post-collision, Chinese Altay, NW China. *Lithos (Oslo)*, **162-163**, 236-250, https://doi.org/http://dx.doi.org/10.1016/j.lithos.2013.01.007.

Gao, J.F., Zhou, M.F., Lightfoot, P.C., Wang, C.Y., Qi, L. and Sun, M. 2013. Sulfide-saturation and magma emplacement in the formation of the Permian Huangshandong Ni-Cu sulfide deposit, Xinjiang, NW China. *Economic Geology*, **108**.

Gole, M.J. and Barnes, S.J. 2020. The association between Ni-Cu-PGE sulfide and Ni-Co lateritic ores and volcanic facies within the komatiites of the 2.7 Ga East Yilgarn Craton Large Igneous Province, Western Australia. *Ore Geology Reviews*, **116**, 103231, https://doi.org/10.1016/j.oregeorev.2019.103231.

Green, A.H. and Melezhik, V.A. 1999. Geology of the Pechenga ore deposits - a review with comments on ore forming processes. *In*: Keays, R.R., Lesher, C.M., Lightfoot, P.C. and Farrow, C.E.G. (eds) *Dynamic Processes in Magmatic Ore Deposits and their Application in Mineral Exploration*. Geological Association of Canada Short Course 13, Sudbury, 287-328.

Griffin, W., O'Reilly, S.Y. and Begg, G.C. 2013. Continental-root control on the genesis of magmatic ore deposits. *Nature GeoScience*, **6**, 905-910, https://doi.org/10.1038/NGEO1954.

Halley, S. 2020. Mapping Magmatic and Hydrothermal Processes from Routine Exploration Geochemical Analyses. *Economic Geology*, **115**, 489-503, https://doi.org/10.5382/econgeo.4722.

Hanski, E. and Smolkin, V.F. 1989. Pechenga ferropicrites and other early Proterozoic picrites in the eastern part of the Baltic Shield. *Precambrian Research*, **45**, 63-82.

Hanski, E., Luo, Z.-Y., Oduro, H. and Walker, R.J. 2011. The Pechenga Ni-Cu Sulfide Deposits, Northwestern Russia: A Review with New Constraints from the Feeder Dikes. *Reviews in Economic Geology*, **17**, 145-162.

Hanski, E., Kamenetsky, V.S. *et al.* 2010. Primitive magmas in the Emeishan large igneous province, southwestern China and northern Vietnam. *Lithos (Oslo)*, **119**, 75-90, https://doi.org/http://dx.doi.org/10.1016/j.lithos.2010.04.008.

Hanski, E.J. 1992. Petrology of the Pechenga ferropicrites and cogenetic Ni-bearing gabbro-wehrlite intrusions, Kola Peninsula, Russia. *Geological Survey of Finland. Bulletin*, **367**, 192.

Hanski, E.J. and Smolkin, V.F. 1995. Iron- And Lree-enriched Mantle Source For Early Proterozoic Intraplate Magmatism As Exemplified By The Pechenga Ferropicrites, Kola Peninsula, Russia. *Lithos*, **34**, 107-125.

Hao, H., Campbell, I.H., Park, J.-W., Cooke, D.R. and Riches, A.J.V. 2017. Platinum group element geochemistry used to determine Cu and Au fertility in the Northparkes igneous suites, New South Wales, Australia. *Geochimica et Cosmochimica Acta*, **216**, 372-392, https://doi.org/https://doi.org/10.1016/j.gca.2017.05.009.

Helz, R.T., Czamanske, G.K. and Zientek, M.L. 1985. Compositions of fine-grained mafic rocks from sills and dikes associated with the Stillwater Complex. *Special Publication - State of Montana Bureau of Mines and Geology*, **92**, 97-117.
Herzberg, C., Asimow, P.D. *et al.* 2007. Temperatures in ambient mantle and plumes; constraints from basalts, picrites, and komatiites. *Geochemistry, Geophysics, Geosystems - G (super 3)*, **8**, @Q02006.
Hicks, J., Barnes, S.J., Le Vaillant, M. and Mole, D. 2017. Savannah nickel sulfide deposits. *In*: Phillips, N. (ed.) *Australian Ore Deposits Monograph*. Australian Institute of Mining and Metallurgy, Melbourne, 435-440.
Keays, R.R. 1995. The role of komatiitic and picritic magmatism and S-saturation in the formation of ore deposits. *Lithos*, **34**, 1-18.
Keays, R.R. and Lightfoot, P.C. 2007. Siderophile and chalcophile metal variations in Tertiary picrites and basalts from West Greenland with implications for the sulphide saturation history of continental flood basalt magmas. *Mineralium Deposita*, **42**, 319-336.
Keays, R.R. and Lightfoot, P.C. 2015. Geochemical Stratigraphy of the Keweenawan Midcontinent Rift Volcanic Rocks with Regional Implications for the Genesis of Associated Ni, Cu, Co, and Platinum Group Element Sulfide Mineralization *Economic Geology*, **110**, 1235-1267, https://doi.org/10.2113/econgeo.110.5.1235.
Kinnaird, J., Hutchinson, D., Schurmann, L., Nex, P. and De Lange, R. Petrology and Mineralisation of the Southern Platreef: Northern Limb of the Bushveld Complex, South Africa. *Mineralium Deposita*.
Kiseeva, E.S. and Wood, B.J. 2015. The effects of composition and temperature on chalcophile and lithophile element partitioning into magmatic sulphides. *Earth and Planetary Science Letters*, **424**, 280-294, https://doi.org/http://dx.doi.org/10.1016/j.epsl.2015.05.012.
Krivolutskaya, N., Makvandi, S., Gongalsky, B., Kubrakova, I. and Svirskaya, N. 2021. Chemical Characteristics of Ore-Bearing Intrusions and the Origin of PGE-Cu-Ni Mineralization in the Norilsk Area. *Minerals*, **11**, https://doi.org/10.3390/min11080819.
Krivolutskaya, N.A., Gongalsky, B.I. *et al.* 2018. Geology of the western flanks of the Oktyabr'skoe deposit, Noril'sk district, Russia: evidence of a closed magmatic system. *Mineralium Deposita*, 611–630, https://doi.org/10.1007/s00126-018-0827-z.
Lassiter, J.C., DePaolo, D.J. and Mahoney, J.J. 1995. Geochemistry of the Wrangellia flood basalt province: Implications for the role of Continental and Oceanic basalt genesis. *Journal of Petrology*, **36**, 983-1009.
Latypov, R., Chistyakova, S., Barnes, S.J. and Hunt, E.J. 2017. Origin of Platinum Deposits in Layered Intrusions by In Situ Crystallization: Evidence from Undercutting Merensky Reef of the Bushveld Complex. *Journal of Petrology*, **58**, 715-761, https://doi.org/10.1093/petrology/egx032.
Latypov, R.M. 2002. Phase equilibria constraints on relations of ore-bearing intrusions with flood basalts in the Noril'sk region, Russia. *Contribution to Mineralogy and Petrology*, **143**, 438-449.
Latypov, R.M., Smolkin, V.F. and Alapieti, T.T. 2001. Differentiation trend and parent melt composition of Ni-bearing gabbro-wehrlite Pechenga intrusions, Kola Peninsula. *PETROLOGY*, **9**, 329- 344.
Latypov, R.M., Chistyakova, S.Y., Namur, O. and Barnes, S.J. 2020. Dynamics of evolving basaltic magma chambers: textural and chemical evolution of cumulates at the arrival of new liquidus phases. *Earth Science Reviews*, **210**, 103388, https://doi.org/10.1016/j.earscirev.2020.103388.
Latyshev, A.V., Veselovskiy, R.V., Fetisova, A.M., Rad'ko, V.A. and Pavlov, V.E. 2020. Correlation of the Permian-Triassic ore-bearing intrusions of the Norilsk region with the volcanic sequence of the Siberian Traps based on the paleomagnetic data. *Economic Geology*, **this issue, in press**.
Le Vaillant, M., Fiorentini, M.L. and Barnes, S.J. 2016. Review of lithogeochemical exploration tools for komatiite-hosted nickel sulphide deposits. *Journal of Geochemical Exploration*, **168**, 1-19, https://doi.org/doi:10.1016/j.gexplo.2016.05.010.
Le Vaillant, M., Barnes, S.J. *et al.* 2020. Multidisciplinary study of a complex magmatic system: The Savannah Ni-Cu-Co Camp, Western Australia. *Ore Geology Reviews*, **117**, 103292, https://doi.org/10.1016/j.oregeorev.2019.103292.
Lesher, C.M. and Barnes, S.J. 2008. Komatiite-associated Ni-Cu-PGE deposits. *In*: Arndt, N.T., Lesher,C.M., Barnes,S.J. (ed.) *Komatiite*. Cambridge University Press, Cambridge, 295-327.

Lesher, C.M., Burnham, O.M., Keays, R.R., Barnes, S.J. and Hulbert, L. 2001. Trace-element geochemistry and petrogenesis of barren and ore-associated komatiites. *Canadian Mineralogist*, **39**, 673- 696.

Li, C. and Naldrett, A.J. 1999. Geology and petrology of the Voisey's Bay intrusion: reaction of olivine with sulfide and silicate liquids. *Lithos*, **47**, 1- 31.

Li, C. and Ripley, E.M. 2011. The giant Jinchuan Ni-Cu-(PGE) deposit; tectonic setting, magma evolution, ore genesis, and exploration implications. *Reviews in Economic Geology*, **17**, 163-180.

Li, C., Ripley, E.M. and Naldrett, A.J. 2009. A new genetic model for the giant Ni-Cu-PGE sulfide deposits associated with the Siberian flood basalts. *Economic Geology*, **104**, 291-301.

Li, C., Tao, Y., Qi, L. and Ripley, E.M. 2012a. Controls on PGE fractionation in the Emeishan picrites and basalts; constraints from integrated lithophile-siderophile elements and Sr-Nd isotopes. *Geochimica et Cosmochimica Acta*, **90**, 12.

Li, C., Arndt, N.T., Tang, Q.Y. and Ripley, E.M. 2015a. Trace element indiscrimination diagrams. *Lithos*, **232**, 76-83.

Li, C., Zhang, M., Fu, P., Qian, Z.Z., Hu, P. and Ripley, E.M. 2012b. The Kalatongke magmatic Ni-Cu deposits in the Central Asian Orogenic Belt, NW China: product of slab window magmatism? *Mineralium Deposita*, **47**, 51-67, https://doi.org/DOI 10.1007/s00126-011-0354-7.

Li, C., Zhang, Z., Li, W., Wang, Y., Sun, T. and Ripley, E.M. 2015b. Geochronology, petrology and Hf-S isotope geochemistry of the newly-discovered Xiarihamu magmatic Ni-Cu sulfide deposit in the Qinghai-Tibet Plateau, western China. *Lithos (Oslo)*, **216-217**, 224-240, https://doi.org/http://dx.doi.org/10.1016/j.lithos.2015.01.003.

Li, C.S., Ripley, E.M. and Naldrett, A.J. 2003. Compositional variations of olivine and sulfur isotopes in the Noril'sk and Talnakh intrusions, Siberia: Implications for ore-forming processes in dynamic magma conduits. *Economic geology and the Bulletin Of the Society Of Economic Geologists*, **98**, 69-86.

Li, X.H., Su, L., Chung, S.L., Li, Z.X., Liu, Y., Song, B. and Liu, D.Y. 2005. Formation of the Jinchuan Ultramafic Intrusion and the World's Third Largest Ni-Cu Sulfide Deposit: Associated With the Similar to 825 Ma South China Mantle Plume? - Art. No. Q11004. *Geochemistry Geophysics Geosystems*, **6**, 11004.

Lightfoot, P.C. and Naldrett, A.J. 1984. Chemical variation in the Insizwa Complex, Transkei, and the nature of the parent magma. *Canadian Mineralogist*, **22**, 111-123.

Lightfoot, P.C. and Keays, R.R. 2005. Siderophile and Chalcophile Metal Variations in Flood Basalts from the Siberian Trap, Noril'sk Region: Implications for the Origin of the Ni-Cu-PGE Sulfide Ores. *Economic Geology*, **100**, 439-462.

Lightfoot, P.C. and Evans-Lamswood, D.M. 2015. Structural controls on the primary distribution of mafic–ultramafic intrusions containing Ni–Cu–Co–(PGE) sulfide mineralization in the roots of large igneous provinces. *Ore Geology Reviews*, **64**, 354-386.

Lightfoot, P.C., Keays, R.R., Evans-Lamswood, D. and Wheeler, R. 2012. S saturation history of Nain plutonic suite mafic intrusions; origin of the Voisey's Bay Ni-Cu-Co sulfide deposit, Labrador, Canada. *Mineralium Deposita*, **47**, 23-50, https://doi.org/http://dx.doi.org/10.1007/s00126-011-0347-6.

Lightfoot, P.C., Naldrett, A.J., Gorbachev, N.S., Doherty, W. and Fedorenko, V.A. 1990. Geochemistry of the Siberian Trap of the Noril'sk area, USSR, with implications for the relative contributions of crust and mantle basalt magmatism. *Contributions to Mineralogy and Petrology*, **104**, 631-644.

Lu, Y., Lesher, C.M. and Deng, J. 2019. Geochemistry and genesis of magmatic Ni-Cu-(PGE) and PGE-(Cu)-(Ni) deposits in China. *Ore Geology Reviews*, **107**, 863-887, https://doi.org/http://dx.doi.org/10.1016/j.oregeorev.2019.03.024.

Luolavirta, K., Hanski, E., Maier, W. and Santaguida, F. 2017. Whole-rock and mineral compositional constraints on the magmatic evolution of the Ni-Cu-(PGE) sulfide ore-bearing Kevitsa intrusion, northern Finland. *Lithos*, **296-299**, 37-53, https://doi.org/https://doi.org/10.1016/j.lithos.2017.10.015.

Maier, W.D., Barnes, S.J. and Dewaal, S.A. 1998. Exploration for magmatic Ni-Cu-PGE sulphide deposits - a review of recent advances in the use of geochemical tools, and their application to some South African ores. *South African Journal of Geology*, **101**, 237- 253.

Maier, W.D., Barnes, S.-J. and Ripley, E.M. 2011. The Kabanga Ni Sulfide Deposits, Tanzania: A Review of Ore-Forming Processes. *Reviews in Economic Geology*, **17**, 217-234.

Maier, W.D., Smithies, R.H. *et al.* 2016. Petrogenesis and Ni-Cu sulphide potential of mafic-ultramafic rocks in the Mesoproterozoic Fraser Zone within the Albany-Fraser Orogen, Western Australia. *Precambrian Research*, **281**, 27-46, https://doi.org/10.1016/j.precamres.2016.05.004.

Mao, Y., Qin, K., Li, C. and Tang, D. 2015. A modified genetic model for the Huangshandong magmatic sulfide deposit in the Central Asian orogenic belt, Xinjiang, western China. *Mineralium Deposita*, **50**, 65-82, https://doi.org/http://dx.doi.org/10.1007/s00126-014-0524-5.

Mao, Y., Qin, K., Li, C., Xue, S. and Ripley, E.M. 2014. Petrogenesis and ore genesis of the Permian Huangshanxi sulfide ore-bearing mafic-ultramafic intrusion in the Central Asian orogenic belt, western China. *Lithos (Oslo)*, **200-201**, 111-125, https://doi.org/http://dx.doi.org/10.1016/j.lithos.2014.04.008.

Mao, Y.J., Barnes, S.J., Duan, J., Qin, K.Z., Godel, B. and Jiao, J.G. 2018. Morphology and particle size distribution of olivines and sulphides in the Jinchuan Ni-Cu sulphide deposit: Evidence for sulphide percolation in a crystal mush. *Journal of Petrology*, **in press**, https://doi.org/10.1093/petrology/egy077.

Mao, Y.J., Barnes, S.J. *et al.* 2022. Sulfide ore formation of the Kalatongke Ni-Cu deposit as illustrated by sulfide textures. *Economic Geology*, **online**, https://doi.org/10.5382/econgeo.4914.

McDonald, I. and Holwell, D. 2011. Geology of the northern Bushveld Complex and the setting and genesis of the Platreef Ni–Cu–PGE deposit. *Magmatic Ni–Cu and PGE deposits: geology, geochemistry, and genesis. Rev Econ Geol*, **17**, 297-327.

McDonough, W.F. and Sun, S.-S. 1995. The composition of the Earth. *Chemical Geology*, **120**, 223-253.

Mole, D., Fiorentini, M.L. *et al.* 2014. Archean komatiite volcanism controlled by the evolution of early continents. . *Proceedings of the National Academy Of Sciences*, **111**, 10083–10088, https://doi.org/10.1073/pnas.1400273111.

Mole, D.R., Barnes, S.J., Taylor, R.J.M., Kinny, P. and Fritz, H. 2017. A Relic of the Mozambique Ocean in south-east Tanzania. *Precambrian Research*, **305**, 386-426, https://doi.org/10.1016/j.precamres.2017.10.009.

Mole, D.R., Barnes, S.J., Le Vaillant, M., Martin, L.A.J. and Hick, J. 2018. Timing, geochemistry and tectonic setting of intrusion-hosted Ni-Cu sulfide deposits of the Halls Creek Orogen, Western Australia. *Lithos*, **314-315**, 425-446, https://doi.org/10.1016/j.lithos.2018.06.017.

Morse, S.A. 1996. KIglapait mineralogy 3. Olivine compositions and Rayleigh fractionation models *Journal of Petrology*, **37**, 1.

Mudd, G.M. and Jowitt, S.M. 2014. A Detailed Assessment of Global Nickel Resource Trends and Endowments. *Economic Geology*, **109**, 1813-1841.

Mungall, J.E. and Naldrett, A.J. 2008. Ore deposits of the platinum-group elements. *Elements*, **4**, 253-258, https://doi.org/10.2113/gselements.4.4.253.

Naldrett, A. 2011. Fundamentals of Magmatic Sulfide Deposits. *Reviews in Economic Geology*, **17**, 1-50.

Naldrett, A.J. 2004. *Magmatic Sulfide Deposits: Geology, Geochemistry and Exploration*. Springer, Heidelberg.

Naldrett, A.J., Keats, H., Sparkes, K. and Moore, R. 1996a. Geology of the Voisey's Bay Ni-Cu-Co deposit, Labrador, Canada. *EXPLORATION AND MINING GEOLOGY*, **5**, 69-179.

Naldrett, A.J., Fedorenko, V.A. *et al.* 1996b. Controls on the composition of Ni-Cu sulfide deposits as illustrated by those at Norilsk, Siberia. *Economic Geology*, **91**, 751-773.

Naldrett, A.J., Fedorenko, V.A. *et al.* 1996c. Controls on the composition of Ni-Cu sulfide deposits as illustrated by those at Noril'sk, Siberia. *Economic geology and the Bulletin Of the Society Of Economic Geologists*, **91**, 751-773, https://doi.org/http://dx.doi.org/10.2113/gsecongeo.91.4.751.

Nielsen, T.F.D., Anderson, J.C.O. *et al.* 2015. The Skaergaard PGE and Gold Deposit: the Result of in situ Fractionation, Sulphide Saturation, and Magma Chamber-scale Precious Metal Redistribution by Immiscible Fe-rich Melt. *Journal of Petrology*, **56**, 643–1676, https://doi.org/10.1093/petrology/egv049.

Pang, K.N., Zhou, M.F., Qi, L.A., Shellnutt, G., Wang, C.Y. and Zhao, D.G. 2010. Flood basalt-related Fe-Ti oxide deposits in the Emeishan large igneous province, SW China. *Lithos*, **119**, 123-136.

Pearce, J.A. 2008. Geochemical fingerprinting of oceanic basalts with applications to ophiolite classification and the search for Archean oceanic crust. *Lithos*, **100**, 4-48, https://doi.org/10.1016/j.lithos.2007.06.016.

Pearce, J.A. 2014. Geochemical fingerprinting of the Earth's oldest rocks. *Geology (Boulder)*, **42**, 175-176, https://doi.org/http://dx.doi.org/10.1130/focus022014.1.

Peters, W.S. 2006. Geophysical exploration for nickel sulfide deposits in the Yilgarn Craton. *Society of Economic Geologists Special Publication 13*, 167-193.

Richards, M.A., Duncan, R.A. and Courtillot, V.E. 1989. Flood basalts and hotspot tracks; plume heads and tails. *SCIENCE*, **246**, 103-106.

Ripley, E.M. and Li, C. 2011. A Review of Conduit-Related Ni-Cu-(PGE) Sulfide Mineralization at the Voisey’s Bay Deposit, Labrador, and the Eagle Deposit, Northern Michigan. *In*: Li, C. and Ripley, E.M. (eds) *Magmatic Ni-Cu and PGE deposits: geology, geochemistry and genesis. Reviews in Economic Geology 17. Reviews in Economic Geology*, Society of Economic Geologists, Littleton, 181-197.

Ripley, E.M., Lambert, D.D. and Frick, L.R. 1998. Re-Os, Sm-Nd, and Pb isotopic constraints on mantle and crustal contributions to magmatic sulfide mineralization in the Duluth Complex. *Geochimica et Cosmochimica Acta*, **62**, 3349- 3365.

Robertson, J.C., Barnes, S.J. and Le Vaillant, M. 2015. Dynamics of magmatic sulphide droplets during transport in silicate melts and implications for magmatic sulphide ore formation. *Journal of Petrology*, **56**, 2445-2472, https://doi.org/10.1093/petrology/egv078.

Santaguida, F., Luolavirta, K., Lappalainen, M., Ylinen, J., Voipio, S. and Jones, S. 2015. The Kevitsa Ni-Cu-PGE deposit in the Central Lapland Greenstone Belt in Finland. *In*: Maier, W.D., Lahtinen, R. and O' Brien, H. (eds) *Mineral Deposits of Finland*. Elsevier, 195-210, https://doi.org/10.1016/B978-0-12-410438-9.00008-X.

Schoneveld, L.E., Barnes, S.J., Williams, M., Le Vaillant, M. and Paterson, D. 2020a. Silicate and oxide mineral chemistry and textures of the Norilsk-Talnakh Ni-Cu-PGE ore-bearing intrusions. *Economic Geology*, **115**, 1227-1243, https://doi.org/10.5382/econgeo.4747.

Schoneveld, L.E., Barnes, S.J. *et al.* 2020b. Zoned Pyroxenes as Prospectivity Indicators for Magmatic Ni-Cu Sulfide Mineralization. *Frontiers in Earth Science*, **8**, https://doi.org/10.3389/feart.2020.00256.

Smithies, R.H., Spaggiari, C.V., Kirkland, C.L., Howard, H.M. and Maier, W.D. 2013. *Melting, mixing, and emplacement; evolution of the Fraser Zone, Albany-Fraser Orogen. GSWA Record 2013/5.* Geological Survey of Western Australia, Perth, West. Aust. Report **0728-2311, 0728-2311**.

Song, X., Zhou, M., Keays, R., Cao, Z., Sun, M. and Qi, L. 2006. Geochemistry of the Emeishan Flood Basalts at Yangliuping, Sichuan, Sw China: Implications for Sulfide Segregation. *Contributions to Mineralogy and Petrology*, **152**, 53-74.

Song, X., Junnian, Y. *et al.* 2016a. The giant Xiarihamu Ni-Co sulfide deposit in the East Kunlun orogenic belt, northern Tibet Plateau, China. *Economic geology and the Bulletin Of the Society Of Economic Geologists*, **111**, 29-55, https://doi.org/http://dx.doi.org/10.2113/econgeo.111.1.29.

Song, X., Yi, J. *et al.* 2016b. The giant Xiarihamu Ni-Co sulfide deposit in the East Kunlun orogenic belt, northern Tibet Plateau, China. *Economic geology and the Bulletin Of the Society Of Economic Geologists*, **111**, 29-55, https://doi.org/http://dx.doi.org/10.2113/econgeo.111.1.29.

Song, X.Y., Wang, K.Y., Barnes, S.J., Yi, J.-N. and Schoneveld, L.E. 2020. Petrogenetic insights of chromite in ultramafic cumulates: Implications from the Xiarihamu intrusion, northern Tibet Plateau, China. *AMERICAN MINERALOGIST*, **105**, 479-497.

Spaggiari, C.V., Kirkland, C.L., Smithies, R.H., Wingate, M.T.D. and Belousova, E. 2015. Transformation of an Archean craton margin during Proterozoic basin formation and magmatism: the Albany–Fraser Orogen, Western Australia. *Precambrian Research*, **266**, 440-466.

Sun, T., Qian, Z., Deng, Y., Li, C., Song, X. and Tang, Q. 2013. PGE and isotope (Hf-Sr-Nd-Pb) constraints on the origin of the Huangshandong magmatic Ni-Cu sulfide deposit in the Central Asian orogenic belt, northwestern China. *Economic geology and the Bulletin Of the Society Of Economic Geologists*, **108**, 1849-1864, https://doi.org/http://dx.doi.org/10.2113/econgeo.108.8.1849.

Tang, D., Qin, K., Su, B., Mao, Y., Evans, N.J., Niu, Y. and Kang, Z. 2020. Sulfur and copper isotopic signatures of chalcopyrite at Kalatongke and Baishiquan; insights into the origin of magmatic

Ni-Cu sulfide deposits. *Geochimica et Cosmochimica Acta*, **275**, 209-228, https://doi.org/http://dx.doi.org/10.1016/j.gca.2020.02.015.

Tao, Y., Hu, R., Qu, W. and Du, A. 2008. Re/Os isotope study of sulfide and olivine pyroxenite in the Limahe nickel deposit, Sichuan, China. *Dizhixue Bao = Acta Geologica Sinica*, **82**, 1292-1304.

Taranovic, V., Ripley, E.M., Li, C. and Rossell, D. 2015. Petrogenesis of the Ni–Cu–PGE sulfide-bearing Tamarack Intrusive Complex, Midcontinent Rift System, Minnesota. *Lithos*, **212-215**, 16-31.

Taranovic, V., Barnes, S.J., Beresford, S.W., Williams, M.J., MacRae, C. and Schoneveld, L.E. 2022. Nova – Bollinger Ni – Cu Sulfide Ore Deposits, Fraser Zone, Western Australia: Petrogenesis of the Host Intrusions. *Economic Geology*, **117**, 455-484, https://doi.org/10.5382/econgeo.4873.

Tegner, C., Thy, P., Holness, M.B., Jakobsen, J.K. and Lesher, C.E. 2009. Differentiation and Compaction in the Skaergaard Intrusion. *Journal of Petrology*, **50**, 813-840.

Wager, L.R., Brown, G.M. and Wadsworth, W.J. 1960. Types of igneous cumulates. *Journal of Petrology*, **1**, 73-85.

Xu, B., Hou, Z., Griffin, W.L., Lu, Y., Belousova, E., Xu, J. and O'Reilly, S.Y. 2021. Recycled volatiles determine fertility of porphyry deposits in collisional settings. *AMERICAN MINERALOGIST*, **106**, 656-661, https://doi.org/https://doi.org/10.2138/am-2021-7714.

Yao, Z.-S. and Mungall, J.E. 2021. Linking the Siberian Flood Basalts and Giant Ni-Cu-PGE Sulfide Deposits at Norilsk. *Journal of Geophysical Research: Solid Earth*, **126**, e2020JB020823, https://doi.org/https://doi.org/10.1029/2020JB020823.

Yao, Z., Mungall, J.E. and Qin, K.Z. 2020. A Preliminary Model for the Migration of Sulfide Droplets in a Magmatic Conduit and the Significance of Volatiles. *Journal of Petrology*, **online**, https://doi.org/10.1093/petrology/egaa005.

Zhang, M., O'Reilly, S., Wang, K.-L., Hronsky, J. and Griffin, W. 2008. Flood basalts and metallogeny: the lithosphere mantle connection. *Earth Science Reviews*, **86**, 145-174.

Zhang, Z., Mao, J., Chai, F., Yan, S., Chen, B. and Pirajno, F. 2009. Geochemistry of the Permian Kalatongke Mafic Intrusions, Northern Xinjiang, Northwest China: Implications for the Genesis of Magmatic Ni-Cu Sulfide Deposits. *Economic Geology*, **104**, 185-203.

Zhao, Y., Xue, C., Zhao, X., Yang, Y., Ke, J., Zu, B. and Zhang, G. 2016. Origin of anomalously Ni-rich parental magmas and genesis of the Huangshannan Ni-Cu sulfide deposit, Central Asian orogenic belt, northwestern China. *Ore Geology Reviews*, **77**, 57-71, https://doi.org/http://dx.doi.org/10.1016/j.oregeorev.2016.02.003.

Zientek, M.L., Bawiec, W.J., Page, N.J. and Cooper, R.W. 1989. Maps, sections, and structure-contour diagrams showing the geology and geochemistry of the Mouat nickel-copper prospect, Stillwater Complex, Stillwater County, Montana. U. S. Geological Survey, 9-9, 2 sheets.